Top Curr Chem (2005) 256: 167–218
DOI 10.1007/b107174

Published online: 1 July 2005

Chirality Effects in Self-assembled Fibrillar Networks

Aurélie Brizard · Reiko Oda · Ivan Huc (✉)

Institut Européen de Chimie et Biologie, 2 rue Robert Escarpit, 33607 Pessac, France
r.oda@iecb.u-bordeaux.fr, i.huc@iecb.u-bordeaux.fr

Abstract Chirality seems to be intimately associated with the growth and stability of self-assembled fibrillar networks and with the most common macroscopic property of these networks, which is the thermoreversible gelation of the solvent. The presence and the relative configurations of stereogenic centers in the structure of a small molecule gelator are generally (but not always) observed to be critical to its ability to form gels. Symmetry considerations of chiral molecular packing provide thermodynamic and kinetic arguments that may explain why chirality favors fiber growth. Additionally, molecular chirality is sometimes expressed at a scale of nanometers or micrometers and gives rise to twisted or coiled fiber structures that are readily observable by microscopic techniques. These chiral fiber morphologies have already found some applications as templates for helical protein crystallization or for the growth of chiral inorganic replicas. The chiroptical properties of assembled chiral molecules, e.g., circular dichroism, allow monitoring of aggregation and may sometimes give insights into molecular packing. But determining chiral molecular arrangements in the fibers remains a challenge and requires the use of multiple techniques.

Keywords Chirality · Gels · Self-assembly · Helices · Fibers

Abbreviations

AFM	Atomic force microscopy
CD	Circular dichroism
DIC	Differential interference contrast
HRSEM	High-resolution scanning electron microscopy
NMR	Nuclear magnetic resonance
SEM	Scanning electron microscopy
STM	Scanning tunneling microscopy
TEM	Transmission electron microscopy
VCD	Vibrational circular dichroism
WAXS	Wide-angle X-ray scattering

1 Introduction

Chirality seems to be intimately associated with the growth and stability of self-assembled fibrillar networks of small organic molecules and with the most common macroscopic property of these networks, which is the thermoreversible gelation of the solvent. The importance of chirality is apparent both at the molecular scale and at the scale of the self-assembled fibers, which typically ranges from nanometers to micrometers. This chapter attempts to review literature data about both these aspects.

As is discussed in the second section of this chapter, many research groups have reported that the presence of at least one stereogenic center in the structure of a small molecule gelator determines its ability to form gels in organic solvents or in water. Molecular chirality thus seems to promote the growth of assemblies with high aspect ratio that entrap the solvent in which they form. When the molecule possesses several stereogenic centers, their relative configuration is also critical to the gelling properties. This has led to the simple empirical (though not general) rule that a molecule has a better chance to be a good gelator if it is chiral. But these observations remain for a large part difficult to explain.

On the other hand, molecular chirality is sometimes expressed at a much larger scale in the morphology of self-assembled fibers. Elongated, fibrous objects such as rods, tapes, or tubes may be helically twisted, coiled, or wound around one another, and therefore exist in a left-handed or a right-handed form. These intriguing shapes can often be simply visualized by microscopic techniques and have fascinated both chemists and physicists. The third section of this chapter aims to illustrate the structural variety of these objects and the extent to which their formation can be altered and their shapes tuned upon changing the experimental conditions. It also gives a perspective of the

relations that can sometimes be drawn between on the one hand, chirality of small molecular components and, on the other hand, supramolecular chirality within their assemblies.

The fourth section of the chapter focuses on the various approaches to experimentally address chirality in self-assembled fibers. The unique chiroptical properties of chiral molecules can be studied by circular dichroism and give access to valuable information about the conformations and relative positions of the molecules in the fibers. This section also gives an overview of the techniques that have been used to observe and assign fiber handedness.

One of the reasons why gels and self-assembled fibers attract so much attention is their very high potential for applications. The last section of this chapter addresses applications which specifically make use of chirality, such as those based on enantioselective molecular recognition, or those based on the use of chiral fibers as templates for the generation of helical arrays of proteins or of chiral inorganic materials.

This chapter was constructed so as to limit overlap with previous reviews on the topic of chirality in self-assembled fibers. Excellent papers by Fuhrhop and Helfrich [1], Schnur [2], and Kunitake [3] were published at the beginning of the 1990s. More recently, an important book chapter appeared about chiral molecular self-assembly of amphiphilic molecules in water or other protic solvents [4]. The present chapter should complement this review in several ways. It extends the field covered to chiral assembly and to gelation in organic solvents. It presents short sections on the tools to investigate chirality in self-assembled fibers and on applications of these chiral fibers. Additionally, the systems are not classified here according to the family of molecules to which they belong, but rather according to the type of properties that they exhibit. This was partly facilitated by the way the field tends to be divided. Indeed, molecular chirality as a factor of gelling ability on the one hand, and chirality expressed in the morphology of the fibers on the other hand, often belong to the same systems. However, many publications tend to focus on one aspect only. Publications dealing primarily with gelling ability describe various aspects which can be considered from the perspective of chirality: the solvent range of gel formation, gel transition temperatures as a function of concentration, possible molecular arrangements of the gelators in the gels etc. These papers often show a few images of the network of fibers, but rarely give detailed accounts of the morphology of these fibers. Conversely, extensive studies about helical or twisted fiber morphology often do not even make mention that the fibers that are studied form a gel.

To further define the scope of this chapter, a line should be drawn between solid fibers and fluid micellar rods [1]. The solid fibers of which organogels and hydrogels are made and which interest us here are generally produced by fast precipitation after having elevated the temperature above the solubil-

ity limit of the gelator. However, fluid-elongated micelles can be produced by simply suspending an amphiphilic molecule in water or, more rarely, in other solvents. Fluid micellar fibers thus exist at temperatures above the solubility limit of the amphiphile (Krafft temperature). Compared to solid fibers, the effect of chirality is rare in fluid fibers [5]. However, the border between these two types of fibers is not always easy to establish. Both may lead to a large increase of viscosity and the visual aspect of the samples can be similar. Moreover, some systems seem to combine both solid and fluid features, for example, the thixotropic gels which spontaneously repair after physical damage.

Formally, physical organogels or hydrogels consist of a network of solid fibers. In other words, connections between the fibers should be necessary to the physical integrity of the gels. But again, this aspect is often not presented in detail in the literature. Micrographs of the samples do not always show clear differences between connected and entangled fibers. Rheological studies should provide definite answers about the importance of connections in a gel, but they are rarely undertaken.

Even with these limitations, the very large body of literature pertaining to the topics presented here could not be covered exhaustively in the context of this chapter. We have selected examples which we thought were illustrative. As a consequence, this chapter is not perfectly representative of the scientific production of the various contributors to this field, and we apologize for any important omissions.

2
Chirality and Gelation

2.1
Most Small Molecule Gelators are Chiral

The number of reports on low molecular mass gelators of organic liquids and water has grown steadily in the last ten years. From this large body of data has emerged an empirical view of the structural requirements for a molecule to gel a liquid. Yet, one is rarely able to predict whether a given molecule will be a gelator. Most new gelator families are still being discovered by serendipity and not by de novo design. A quick look at the literature on small molecule gelators and, to start with, at review articles on this topic makes it clear that the ability to form gels is often associated with the presence of stereogenic centers in the gelator molecular structure [6, 7]. The fact that chirality enhances gelling ability has been persistently (although hardly conclusively) reported. It has become a widely accepted fact and seems to be true for most families of gelators no matter how different they may be

from each other. On the other hand, no broad explanation has yet been proposed. In this section, we have tried to give a clear perspective on the extent to which chirality matters in gelation. We have gathered and organized data from a number of publications, and derived from them hypotheses on the role of chirality in gelation phenomena. Given the large body of literature that pertains to this subject, we did not intend to make an exhaustive presentation and have selected relevant examples. It should be added that our sampling of chiral gelators is not necessarily representative of the numerous families of chiral gelators. Several of these families are derived from steroid derivatives or from complex sugars [6]. In these cases, the synthetic chiral precursors of the gelators are obtained from the chiral pool of natural products, and are often available only as a single enantiomeric form. Neither the racemate nor the other enantiomeric form is readily available. Because of this, the gelling properties of these compounds have not always been addressed from the perspective of chirality and are not accounted for here, even though these gelators are chiral as well. The chiral gelators that are mentioned here are limited to those for which the property of gelation has been addressed in one way or another from the perspective of chirality.

As stated above, the vast majority of gelators possess at least one stereogenic center in their structure. On the contrary, Scheme 1 shows 11 examples of gelators that possess none: chirality is a common but not a universal feature of organic gelators [8–18]. These nonchiral compounds were discovered by different authors in different contexts. Nevertheless, several of them are structurally related. These 11 examples may in fact be reduced to a smaller number of subclasses, such as compounds **1–4**, which all consist of two alkylamido or alkylurea units connected directly or by an aliphatic spacer, C_3 symmetrical tris-amides such as **5** and **7**, and alkoxy-aromatics such as compounds **8** and **9**. In short, the number of families of achiral gelators may be limited to just a few. It is interesting to note that compounds **1–11** gel organic liquids and that none of them gels water. A recent review on water gelation by small organic molecules [7] actually shows that almost all hydrogelators are chiral. As mentioned in the Introduction, a clear distinction should be made between genuine gels, which consist of solid-like fiber networks, and the highly viscous solutions of cylindrical micellar aggregates of amphiphilic molecules [1]. The latter may have a gel-like aspect because of their high viscosity and viscoelasticity but they differ fundamentally from a gel in that they exist at temperatures above the Krafft temperature, and in that they can flow, albeit slowly. This distinction is important because cylindrical micelles seem to form regardless of the presence of stereogenic centers in the amphiphile, and most of the studied micellar cylinders are made of achiral molecules (e.g., cetyltrimethylammonium salicylate [19], or many classes of gemini surfactants [20]).

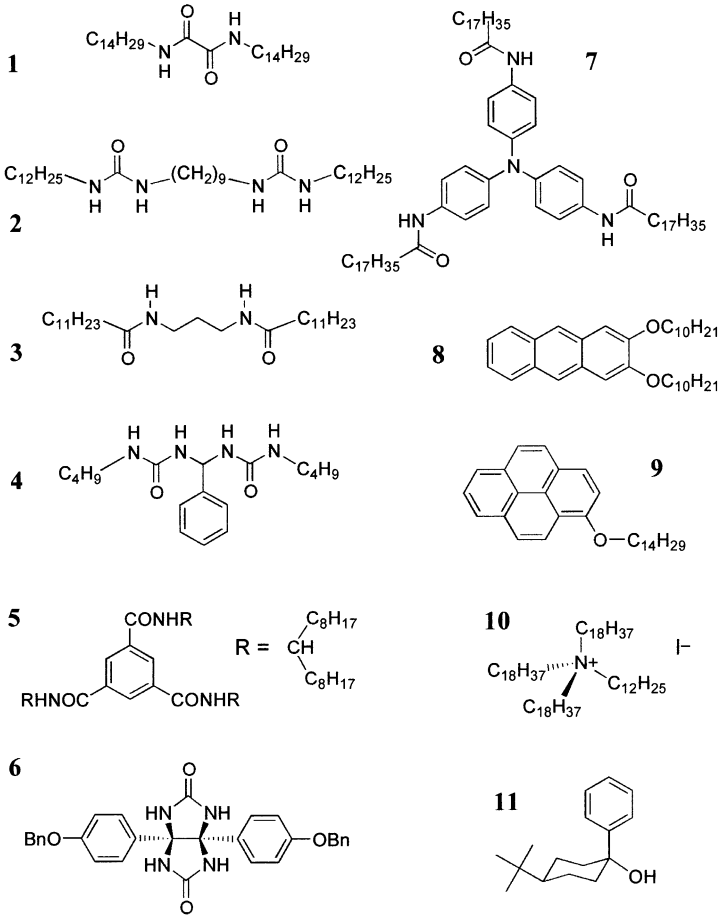

Scheme 1 Representative examples of nonchiral gelators. Compounds **1**–**11** are described in [8–18], respectively.

2.2 Diastereomers Show Different Gelation Behaviors

When a small molecule gelator contains more than one stereogenic center, the various diastereomers may show completely different gelation behaviors. Changing the configuration of a single stereocenter in such a molecule may have dramatic effects on its solubility properties, the range of solvents that can be gelled, the stiffness of the gels it forms, its critical gelation concentration, and the temperature at which its gels melt. The most compelling example of such effects is displayed by 11 isomers of methyl 4, 6-*O*-benzylidene monosaccharides described by Shinkai et al. (Scheme 2) [21, 22]. Among them, only **12a**, **12b**, **12f**, **12i**, and **12j** are good gelators. A closer look at

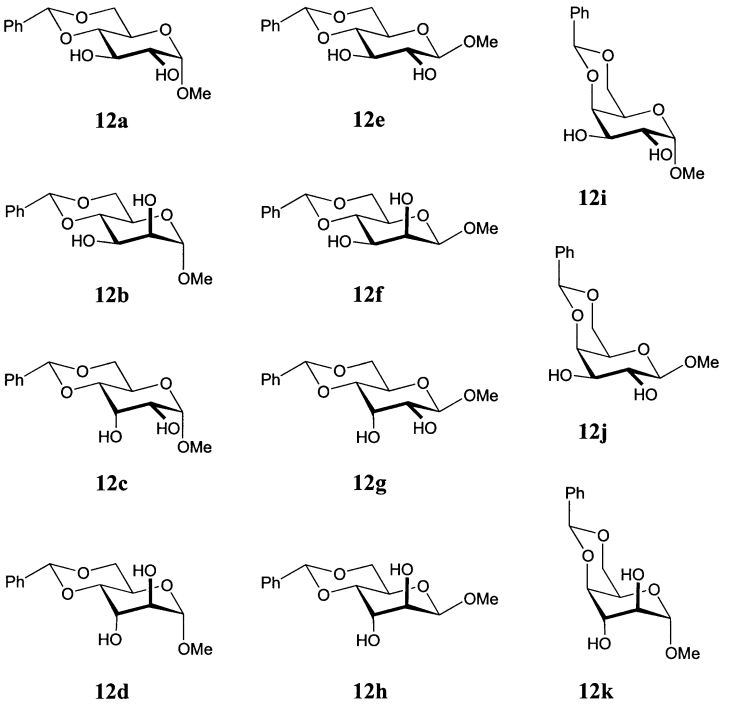

Scheme 2 Methyl 4, 6-*O*-benzylidene monosaccharides as gelators [21, 22]

these structures allows one to conclude that efficient gelation—though not necessarily in the same solvents—is possible for both α and β anomers, with equatorial benzylidene groups (*gluco*-**12a** and *manno*-**12b**) and also with axial benzylidene groups (*galacto*-**12i**). No particular configuration appears to prevent gelation by itself, except maybe the axial configuration of the 3-OH group in the *allo*- (**12c**, **12f**), *altro*- (**12d**, **12h**), and *ido*-pyrranosides (**12k**). The nongelators either yield poorly soluble material which precipitates instead of forming gels, or very soluble material which remains soluble at concentrations much above the critical gel concentrations of the gelators. These variations are difficult to predict but can to some extent be rationalized on the basis of the X-ray crystallographic structures of some of these compounds. In the solid state, gelators tend to show one-dimensional arrays of intermolecularly hydrogen bonded molecules. Compounds that are poorly soluble show two-dimensional arrays of intermolecularly hydrogen bonded molecules. And, in one example, exclusively intramolecular hydrogen bonds seem to correlate with high solubility.

In the specific case of *meso* compounds, the gelling properties of chiral and achiral diastereomers can be generalized. Many gelators have a C_2 symmetrical structure and contain two chiral units with the same stereochemistry (Schemes 3 and 4). It is not clear whether such C_2 symmetrical structures

have higher chances to be good gelators, or whether more of them have been found because they are generally easier to prepare in a convergent fashion. Among this rather large family of chiral gelators, we could not find a single example where the achiral *meso* diastereomer is also a gelator. Whenever the *meso* compounds are mentioned in the literature, they invariably tend to form precipitates or crystallize.

2.3 Enantiomerically Pure Gelators Overrun their Racemates

The fact that the presence of a stereogenic center is essential to the gelation properties of a small organic molecule is often characterized by the observation that pure enantiomers of a given gelator have a better ability to form gels than their corresponding racemate. For example, Scheme 3 shows structures which, taken as a single enantiomer, are found to be good gelators, whereas their racemates are reported not to form any gel at all, or at best to form weak, partial, or unstable gels, or to form gels in a restricted range of solvents [23–31]. Again, it should be kept in mind that these examples are not representative of the numerous chiral gelators, but are cases that have been studied from the perspective of chirality. Because they are poor gelators, the properties of the racemates are often considered to be of lesser importance. Few reports described them in detail, and most reports do not mention anything about them. When information about the nature of the aggregates formed by the racemates is available, they are reported to crystallize, or to precipitate as flakes or platelets. Thus, when the two enantiomers of a gelator are mixed two phenomena result. First, they generally combine in a single aggregate. Second, this aggregate differs significantly in size and aspect ratio from the gel fibers of the single enantiomer, and does not lead to a gel.

The tendency of enantiomeric gelators to coaggregate is nicely illustrated by the results of van Esch et al. [29] who showed that the probe (*S*, *S*)-**19b** with its azobenzene chromophores (Scheme 3) has a marked preference to be incorporated in the gel fibers of (*R*, *R*)-**19a**, which possesses an opposite chirality, rather than in the gel fibers of (*S*, *S*)-**19a**, which has the same chirality. Other interesting examples were provided by Fuhrhop et al., who showed that the two enantiomers of gluconamide **18** [28] coaggregate in platelets even when they possess alkyl chains of different lengths [32].

Coaggregation of enantiomers thus appears to be a common behavior of racemic mixtures of chiral gelators. Yet, there are also rare examples where a racemic gelator forms a conglomerate: the two enantiomers spontaneously resolve into gel fibers consisting of a single enantiomer. The fibers obtained from the racemates and, presumably, from a mixture of the two enantiomers in any proportions are then of an identical nature to the fibers obtained from a pure enantiomer. What varies is only the proportion of fibers containing one enantiomer and of fibers containing the other enantiomer. This was demon-

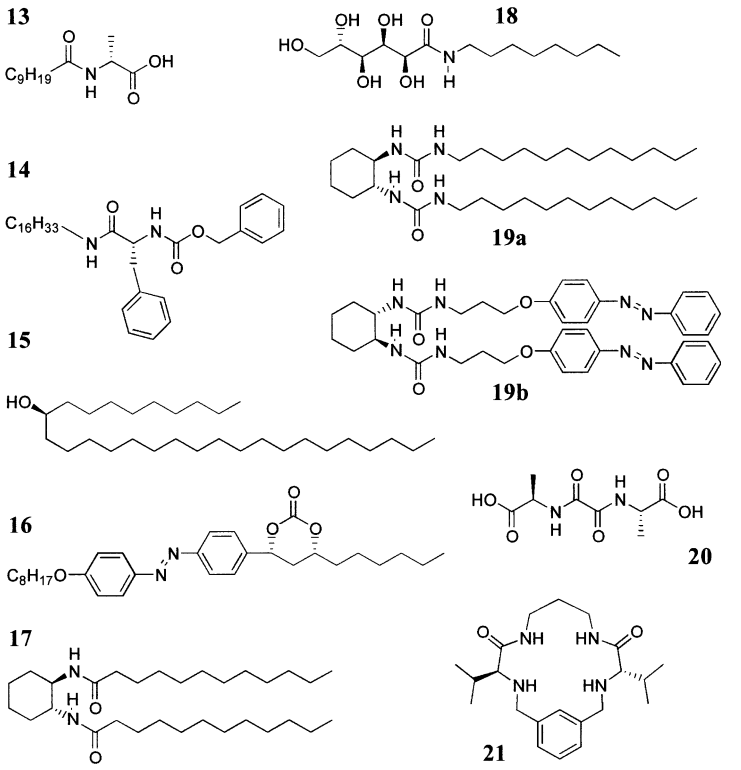

Scheme 3 Gelators that gel as a single enantiomer. Compounds **13–21** are described in references [23–31], respectively

strated unambiguously by calorimetric studies and a phase diagram of mixtures of the two enantiomers of diacetylenic phospholipid **22** (Scheme 4) [33]. It is also supported by circular dichroism studies [34]. A similar phase separation was also proposed in the case of the mixture **27a**+**27b** (Scheme 4) [35]. Right-handed helical fibers are observed in gels of L-**27a**+L-**27b**, left-handed helical fibers form in gels of D-**27a**+D-**27b**, and both right- and left-handed fibers are observed in *rac*-(**27a**+**27b**). Similar results were reported for compound **28** [36]. When such separation between the enantiomers occurs, the racemate forms gels similar to those of the individual enantiomers. But it has also been proposed that even when a conglomerate forms, the presence of the other enantiomer may slow down the formation of the fibers and possibly alter their shapes and thus the properties of the gel [31].

Compounds **23–26** (Scheme 4) exhibit an even less conventional behavior. As for compounds **13–21**, they are good gelators as single enantiomers and their racemic solutions produce racemic aggregates. However, unlike compounds **13–21**, the racemic aggregates of **23–26** have equal or better gelling properties than the single enantiomers. Because of this unusual property,

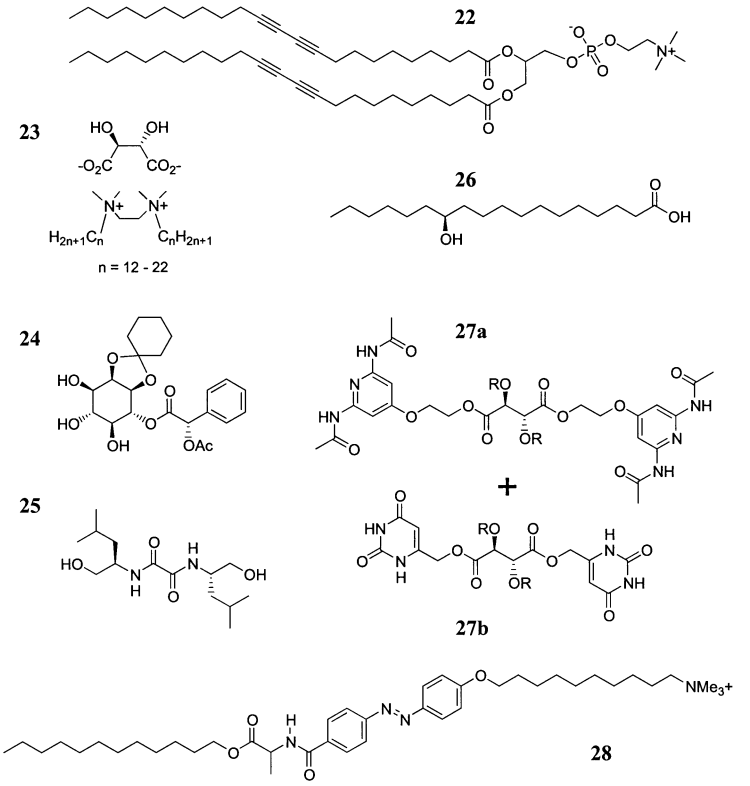

Scheme 4 Gelators that gel as racemates, conglomerates, or solid solutions

these racemates have been the object of detailed studies. For example, Terech et al. clearly established that the racemic gels of 12-hydroxyoctadecanoic acid **26** [37] are comparable in every respect to the gels of the single enantiomer: the aspect of the samples; the concentration range and the range of solvents in which the gels form; the longevity of the gels; the viscosity and viscoelasticity of the gels; the shape of the gel fibers; and the molecular packing within the fibers. In toluene, gelator **24** [38] is able to gel a volume three times as large as a racemate than as a pure enantiomer. Similarly, gelator **25** [39] gels larger volumes (up to ten times) of a variety of solvents as a racemate, and even as a mixture of diastereomers, than as a single enantiomer. For both **24** and **25**, transmission electron microscopy (TEM) shows that the fibers produced by the racemates are thinner, more numerous, and more connected than those produced by the single enantiomer. This is consistent with their ability to gel larger volumes of solvent and contrasts strongly with the large aggregates normally produced by racemates. In a recent publication, Žinić et al. systematically compared the gelation properties of the single enantiomers and of the racemates of eight gelators derived from various amino acids [40]. As ex-

pected, most of the racemates were found to be poor gelators. However, some proved able to gel significantly (up to 16 times) larger volumes of solvents, as for **24** and **25**. Thus, the fact that racemates are poorer gelators cannot be taken as a general rule.

Gelator **23** [41] shows a slightly different behavior. In chlorinated and organic solvents, its racemate forms a crystalline precipitate of large aggregates as for compounds **13–21**. In water, however, its racemate forms stiffer gels than the single enantiomer. TEM studies show that the racemate consists of large platelets, as do most racemates, but these still have a high aspect ratio, and are thicker, wider, longer, and have larger junction zones than the fibers formed by a single enantiomer. Another unusual aspect of this gelator is that the two enantiomers mix in the same gel fibers in any proportions [42], as in a solid solution (a crystal in which the two enantiomers may differently occupy the same crystallographic position [43]). The shape and size of the fibers vary with the enantiomeric excess, but a hydrogel is formed in all cases.

2.4 Comparing Racemic or Homochiral Gel Fibers to Racemic or Homochiral Crystals

The general tendency of both enantiomers of a chiral gelator to aggregate together in racemic fibers is an illustration of their crystalline nature. Indeed, about 90–95% of racemic solutions produce racemic crystals, and at most 5–10% spontaneously resolve in crystals containing exclusively one or the other enantiomer (conglomerate) [43]. In this respect at least, gel fibers seem to behave similar to crystals. The actual physical origin for the preferential formation of crystalline racemates is not yet settled and is still being debated. As early as 1885, it was observed that racemic crystals were generally denser [44, 45]. This higher density was presented as arising from lower values of crystal network free energy. Statistical arguments have also been invoked involving the larger number of nonchiral space groups and the additional symmetry elements that they offer. Racemates have more possibilities of packing than conglomerates. The chances are thus higher that the most stable arrangement lies among racemic packing. More specifically, it can be observed that crystal packing of organic molecules is often guided so as to avoid energetically unfavorable mutual orientations of juxtaposed polar groups of neighboring molecules related by symmetry elements. Thus, a glide reflection is preferable to a pure reflection, a screw rotation is preferable to a pure rotation, and the combination of glide reflection and screw rotation is preferable to either individually [45, 46]. This is reflected by the symmetry properties of the most common achiral space groups ($P2_1/c$, $C2/c$, and $P1$ account for about 85% of the space groups of crystalline racemates) [43] and also by the most common chiral space groups ($P2_1$ and $P2_12_12_1$ account for about 85% of the space groups of organic crystalline enantiomers) [43].

Achiral space groups offer the symmetry elements available in chiral space groups and also additional possibilities (glide reflections and inversion centers), which may lead to a preference for racemic crystals over conglomerates. Finally, kinetic arguments may be involved in the process of forming a viable crystal nucleus from a racemic solution. For a racemic crystal, all molecules (both enantiomers) may find a suitable binding site on the surface of the nucleus, whereas for a conglomerate half of the molecules may scroll on a wrong subcritical cluster belonging to the other enantiomer and inhibit its growth.

These arguments were developed for crystals, but their validity probably extends largely to gel fibers. Though they consist in metastable structures, gel fibers most often give powder diffraction data that reveal a long-range crystal-like order. The various factors presented above may thus shed some light on the fact that racemic gelators tend to coaggregate. However, it remains to explain why these racemates generally do not lead to a gel. Gel fibers arise upon a strong preference for anisotropic unidirectional growth. Instead, racemates aggregate as platelets or crystals, which result from a preferential bidirectional growth or from three-dimensional growth, respectively. Again, it is likely that symmetry considerations come into play in this process. As mentioned above, crystal packing of organic molecules is often guided so as to avoid energetically unfavorable mutual orientations of juxtaposed polar groups of neighboring molecules related by symmetry elements. Since racemic crystals possess additional symmetry elements to limit these repulsions (hence their stability), one can conceive that crystal growth along the various (*hkl*) crystallographic directions has more chances to be even. On the contrary, crystals of a single enantiomer lack some of these symmetry elements, and attractive or repulsive interactions have more chances to be unevenly distributed along the crystallographic directions.

The few examples of chiral gelators that have been characterized by single-crystal X-ray crystallography tend to support this view. This is the case for the example of gelator **25** [38] (Scheme 4), the crystal of which reveals strong directional interactions along the *b* plane and much weaker interactions along the *a* and *c* planes, suggesting an anisotropic growth into fibers. As pointed out by the authors, this rationale relates to the theory of crystal growth proposed by Hartman and Bennema which states that "the relative growth rate of a crystal face increases with E_{att}, which is the energy per molecule released when one slice of thickness d_{hkl} crystallizes onto a crystal face (*hkl*)." Other examples of crystal structures of chiral gelators (or closely related analogues) also show distinct unidirectional arrangements of the molecules. This includes a chiral analogue of **9** [16] (Scheme 1); 4,6-*O*-benzylidene monosaccharides [21, 22] (Scheme 2); a derivative of **16** [26] having shorter alkyl chains (Scheme 3); the bis(valine) analogue of bis(alanine) derivative **20** [30, 47] (Scheme 3); analogues of gelator **21** (Scheme 3) [31], di(*p*-toluyl)-L-cystine [48], sugar-based bolaamphiphiles [49], or a tetralin derivative [50].

It should be added that the most common chiral space groups ($P2_1$ and $P2_12_12_1$) feature twofold screw axes which, by construction, represent columnar arrangements. The crystal structures referred to above belong to these space groups. The unidirectional arrangements of the molecules do not always match a twofold-symmetry screw axis: weak intermolecular interactions may be observed along the 2_1 axis whereas much stronger interactions are observed along another direction. However, some families of molecules have been identified where the 2_1 axis does indeed represent the direction where the strongest intermolecular interactions take place in the crystal, thus defining this crystallographic direction as the direction of most favorable growth. This is the case, for example, in salts of chiral primary amines and achiral carboxylic acids [51].

When considering gel fiber growth, kinetic factors should also be invoked. Despite their crystalline nature, gel fibers are produced out of equilibrium, and are not true, thermodynamically stable crystals. The typical conditions of formation of a gel consist of dissolving the gelator at high temperature and letting it cool upon standing, or upon cooling it actively to accelerate the temperature drop. It has been noted that very slow cooling of the gelator solution may promote crystallization or precipitation instead of gel fiber growth [52]. Conversely, some racemic solutions of gelators may produce gels when cooled very rapidly, whereas simply standing at room temperature leads to weak gels or precipitates [31]. Clearly, the change in temperature has to be commensurate with the energetic factors which promote growth of a gel fiber in a particular direction.

Finally, the fact that gel fibers are not at equilibrium raises the question of what prevents their rearrangement into crystals. Again, it is possible that chirality comes into play. Fuhrhop et al. proposed a rationale to explain the stability of chiral fibers called the "chiral bilayer effect." They predict that the kinetic barrier to rearrange a chiral micellar cylinder into an enantiopolar crystal should be larger than the barrier to rearrange an achiral micellar cylinder into an achiral crystal having a bilayered structure [28]. The generality of this concept has been questioned and it was suspected that its application is limited to amphiphilic structures in aqueous medium [37]. It seems to us that the enantiopolar lamellar structure proposed for crystals of single enantiomers is far from being general. Some chiral gelators show distinct bilayer structures in the solid state [38].

Perhaps an important factor that contributes to the stability of fibers of chiral gelators is their ability to adopt morphologies that express chirality at a mesoscopic scale, giving rise to fibers possessing complex superstructures, such as helical cylinders or multiple helices. As is presented in more detail in the next section, the width of these structures cannot grow without perturbing the molecular packing, thus stabilizing the high aspect ratio of the fibers. Moreover, twisted or helical fibers are less prone than flat objects to forming

thick bundles that would eventually precipitate, because the contact surface involved in a stack of helices is limited compared that of a stack of flat objects.

3
Chirality and Fiber Morphology

When chiral molecules self-assemble into fibrillar structures, chirality is sometimes expressed in the morphology of the fiber at a supramolecular scale of nanometers or micrometers. Elongated objects may be coiled or twisted and exist as a left-handed or a right-handed form. The two enantiomers of the chiral molecule individually generate fibers with opposite handedness but for rare exceptions, or unless they are mixed. This section presents in detail the diverse morphologies of chiral fibers that can be generated, as well as the various means by which these morphologies can be tuned. The last part of this section briefly discusses chiral molecular organization in self-assembled fibers and the mechanisms through which chirality may be expressed at a mesoscopic scale.

As mentioned in the Introduction, literature reports concerning chirality in self-assembled fibers often do not make mention of whether the fibers studied belong to true physical gels or to fibrous precipitates as, for example, in references [2, 53–60]. However, this distinction is not essential when discussing fiber morphology. Gel formation is often a consequence of inhibited crystallization or precipitation. It is generally a strongly history-dependent process and the same solution may produce a fibrous precipitate or a gel depending on how it is treated. However, even though the aspect of the samples may seem different, it is often assumed that the local supramolecular organizations in gel fibers and in fibrous precipitates are very similar.

3.1
Various Chiral Morphologies of Fibrillar Aggregates

Self-assembled fibrillar objects, such as rods, tapes, or tubes, may be helically twisted, coiled, or wound around one another to give multiple helices or even coiled coils. These structures are intrinsically chiral and thus possess a right- or left-handedness. The length, the diameter, and the chiral pitches of the fibers are highly variable: from ~10 nm to 1 mm. The observation that aggregates of chiral molecules may exhibit supramolecular chirality was first reported with natural lipids such as sodium deoxycholate [61], deoxycholic acid [62], and hydroxystearic acid **26** (Scheme 4) and its salts [37, 58, 59]. The D and L enantiomers of hydroxystearic acid were used to provide the first evidence that the handedness of the helical fibers is determined by the configuration of the molecular component. The L enantiomer gives right-handed

twisted fibers, whilst the D enantiomer gives left-handed twisted fibers. Almost 15 years later, the first examples of synthetic chiral molecules forming chiral aggregates were reported [53, 55, 63].

Among the variety of chiral fibrillar structures encountered in the literature, probably the most commonly described are chiral ribbons of single or multiple bilayer membranes. Such ribbons can be roughly classified into two different morphologies: helical and twisted shapes. The distinction between helical and twisted ribbons is shown in Fig. 1. Helical ribbons have a cylindrical curvature and can be precursors of tubules (see below). By comparison, twisted ribbons have Gaussian or saddle-like curvature. Typical examples of helical ribbons are those formed by diacetylenic lipids such as **22** (Scheme 4) [2, 53, 54, 60], by *N*-octyl-L-galactonamide [64], by cytidine myristoylphosphatidyl conjugates [65], or by some chiral single-chain ammonium amphiphiles [66]. Typical examples of twisted morphologies are those of hydrostearic acid [58, 59], of double-chain ammonium amphiphiles derived from glutamic acid [63], or of diammonium cationic gemini surfactants **23** (Scheme 4) [41, 43].

The distinction between twisted and helical chiral morphologies is not always straightforward, and ribbons having both a twisted and a helical component can also form. Additionally, authors do not always use the same nomenclature and term as "helical" ribbons that are actually twisted and vice versa. Why some ribbons have a cylindrical curvature whereas others have a saddle-like shape is still a matter of debate. A theoretical model treating the energy differences in the two types of curvatures has been introduced and it was suggested that for fluid membranes, twisted ribbons are favored, whereas crystalline molecular organization imposes a helical curvature [43, 67]. But this may not be general and is not always verified at the experimental level [67, 68].

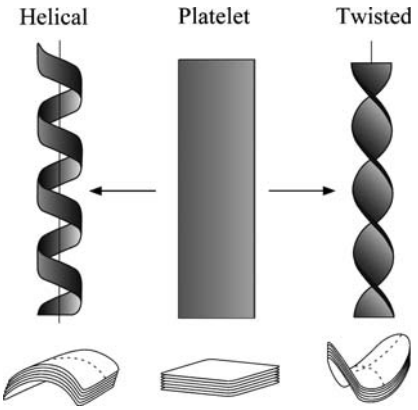

Fig. 1 Schematic representation of helical and twisted ribbons

The expression of molecular chirality at the level of the fiber and the emergence of helical or twisted shapes presumably play a role in the high aspect ratio of the fibers and in the ability of chiral compounds to form gels (see Sect. 2). For example, whilst the width of a flat ribbon may grow infinitely, the width of a helical ribbon is limited to the point when the ribbon transforms into a tubule (see below). The growth in width of a twisted ribbon is also predicted to be limited. For a given pitch of a twisted structure, the tear stress of the edges increases with the width of the ribbon. Despite its edges exposed to the solvent, a twisted ribbon is predicted to reach a finite width that is inversely proportional to the strength of the chiral effect [42].

Helical and twisted ribbons formed from self-assembled chiral amphiphilic molecules may have a single or a multiple bilayer structure. Some have been shown to consist of interdigitated bilayers [69, 70]. Interdigitation is considered to have a consolidation effect for such membrane structures as it results in highly ordered packing. In a few cases, helical ribbons have been shown to wind around one another and generate well-organized multiple helices. This is the case, for example, for gluconamide **18** [28] (Scheme 3). After numerical treatment, the microscope images of the fibers show a spectacular helix comprising four ribbons (Fig. 2) [71, 72].

The various ribbons presented above consist of amphiphilic molecules arranged in bilayers. The long axis of the molecules is perpendicular to the ribbon plane or slightly tilted from this direction. But ribbons or tapes can also be formed from the assembly of molecular rods oriented with their long axis parallel to the width of the ribbon. This is the case for some peptides that form extended β-sheet tapes which stack to form chiral superstructures (Fig. 3) [73]. It is also the case for numerous gelators consisting of a central aromatic core and chiral cholesteryl saccharidic moieties on the sides, such as the porphyrin derivative shown in Fig. 4 [74]. Chirality effects in these

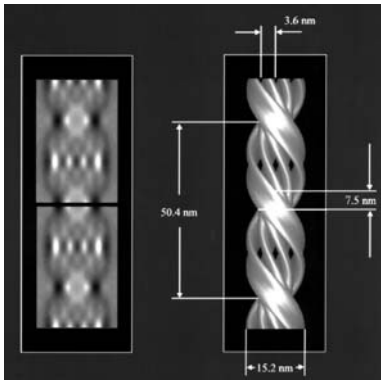

Fig. 2 Electron micrograph of *N*-octyl-D-gluconamide self-assembled fibers and 3D model of four entwined ribbons [71, 72]. Image kindly provided by Dr. Böttcher

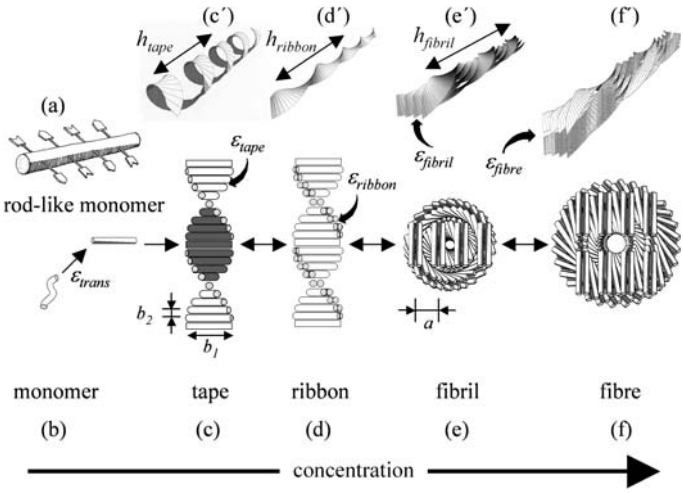

Fig. 3 Model of hierarchical self-assembly of chiral rodlike units. Local arrangements (c–f) and the corresponding global equilibrium conformations (c′–f′) for the hierarchical self-assembling structures formed in solutions of chiral molecules (a), which have complementary donor and acceptor groups, shown by arrows, through which they interact and align to form tapes (c). The black and white surfaces of the rod (a) are reflected in the sides of the helical tape (c), which is chosen to curl toward the black side (c′). The outer sides of the twisted ribbon (d), of the fibril (e), and of the fiber (f) are all white. One of the fibrils in the fiber (f′) is drawn in a darker shade for clarity. (e) and (f) show front views of the edges of fibrils and fibers, respectively. Reprinted with permission from [73]. Copyright 2001 National Academy of Sciences USA

tapes leads to a tilt between each consecutive rod which eventually produces a long-range twist.

Although a cylinder possesses no apparent chirality, chirality may play a role in the formation of cylindrical (tubular) fibers. As seen in Fig. 5, helical ribbons may spontaneously evolve into tubules upon an increase of their width. Tubules that are formed through this pathway often bear helical scars, where the edges of the ribbons have merged, as an indication of their chiral origin. Depending on the experimental conditions, this may be the case for the tubules of diacetylenic lipid **22** (Scheme 4) [2]. Some tubes, however, are produced from vesicles and show no apparent chirality even though the amphiphiles they are made of are chiral [75]. Sometimes, tubular structures form upon rolling up a sheet to form a cigar-like object [64]. As rolling does not occur parallel to the edge of the sheet, the cigar has a right- or left-handedness which may reflect the chirality of the molecular components. Rolling up a sheet is one of the very few possibilities to produce fibers—and potentially gels—from molecules that have no spontaneous tendency to assemble into elongated structures.

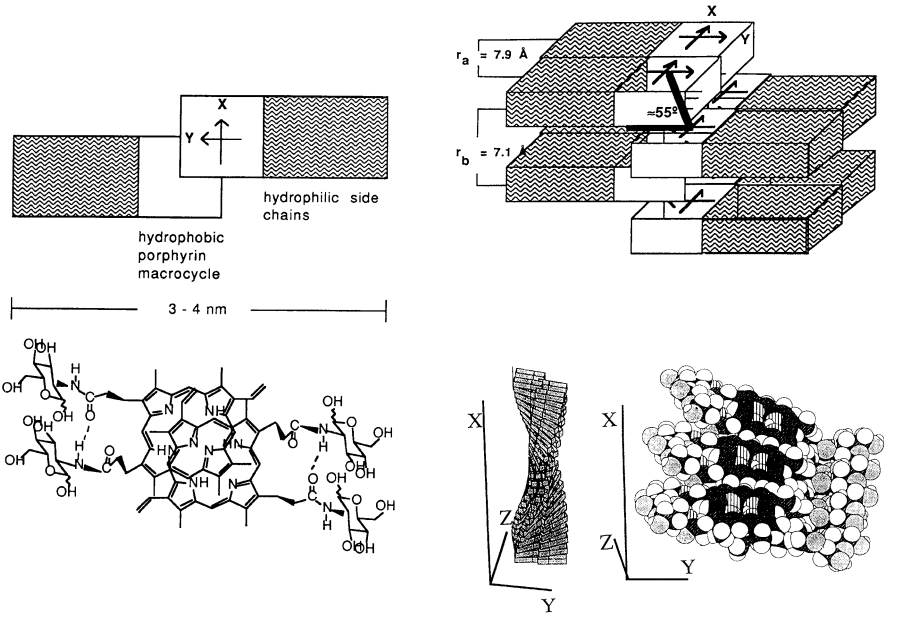

Fig. 4 Proposed twisted ribbons consisting of octametric units of porphyrins bearing aminoglycosamide functions. Reprinted with permission from [74]. Copyright 1992 American Chemical Society

Whilst tubules are hollow fibers, rodlike fibers with no hollow may also reveal the chirality of their molecular components at a mesoscopic scale. However, rodlike fibers are often very thin and structurally more difficult to

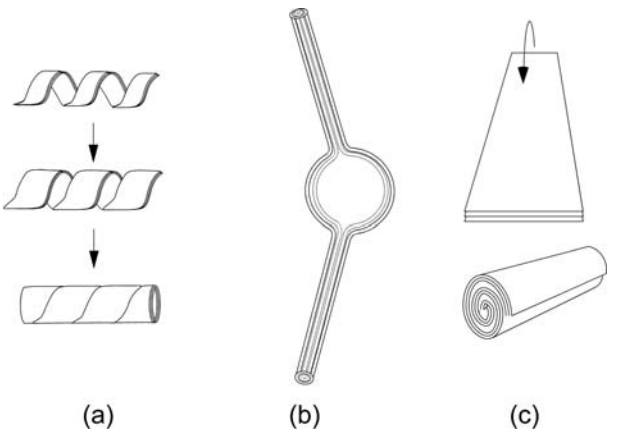

Fig. 5 **a** Helical bilayer growing to form tubules, **b** tubules growing from vesicles, and **c** a planar bilayer sheet rolling up directly to form a cigar-like structure

characterize than fibers derived from ribbons or tapes. Thin fibers tend to wind into bundles in which a global helicity is detected. Some of these fibers supposedly have a cylindrical micellar-type structure with a chiral (helical) solid-like molecular packing (Fig. 6) [64, 65, 76], in contrast to the more usual fluid nature of cylindrical micelles [19, 20]. Fibers may also be formed from stacks of disklike objects such as large aromatic groups which pile up to form a rod. A clockwise or counterclockwise staggering of the disks in the fibers may then give rise to a left-handed or right-handed twist [77]. Both chiral micellar fibers and chiral stacks of disks can wind together to form multiple helices (Fig. 6) and thus generate a second level of helicity (coiled coil). The handedness of such a multiple helix is a function of the handedness of the individual chiral fibers and of various parameters, such as the inclination and depth of the grooves of the chiral fibers. In practice, it is often observed that the multiple helix has a handedness opposite to that of the chiral fibers it is made from [77], as in the coiled coils of some proteins, e.g., keratin. Many other chiral rodlike fibers have dimensions much larger than the diameter of micelles (a few tens of nanometers), and the exact nature of molecular packing in these is far from obvious.

The various chiral fiber morphologies presented above are characterized by long-range helicities which are directly observable by microscopic techniques. These techniques have their own detection limits, and the fact that chirality is not observable in micrographs does not mean that there is no chiral twist within the molecular packing. Indeed, chiral packing can be revealed by spectroscopic methods or even by X-ray crystallography, without necessarily being visible by microscopy. Numerous fibers show intense circular dichroism bands that are not observed in the sol states and that can be interpreted as arising from chiral packing of the molecules (see Sect. 4), even

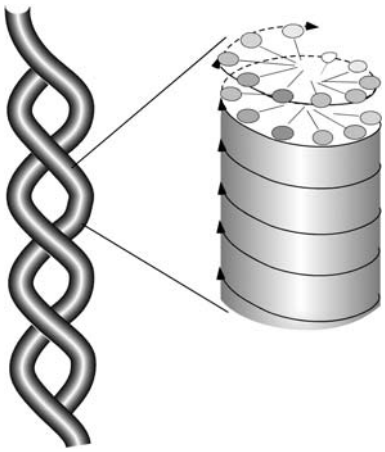

Fig. 6 Micellar fibers with chiral packing of amphiphilic molecules

though no specific chiral morphology is observed. For example, intense induced circular dichroism was observed for L-glutamic acid derivatives [78], various cholesteryl derivatives [79, 80], or oxidized glutathione [81]. Examples of helical organizations revealed by X-ray crystallography have been mentioned in Sect. 2.4 (e.g., references [48] and [50]). Note that in crystals, helical organizations are most commonly simple twofold screw axes. The scale of the helical pitch is then on the order of a few molecules, which is very small compared to the pitches that can be reached in the chiral fibers described above. It is interesting to observe that some fibers may possess both a local crystal-like order and a long-range helical order.

3.2 Morphology Control of Chiral Fibers

It is not easy to predict what parameters cause a chiral gelator to assemble into one type of chiral fiber or another. Very often, the balance between these parameters is subtle, and seemingly slight changes in the experimental conditions may lead to important changes of chiral fiber morphology. For instance, the nature of the solvent, the cooling rate of the sample, or the age of the sample may strongly affect fiber morphology. In addition to these environmental parameters, the most critical is the molecular structure of the amphiphile, within which very slight changes may lead to completely different aggregate morphologies.

The effect of the solvent on chiral fiber morphology can be very strong, but is unfortunately very difficult to rationalize. In some systems, a gelator may assemble into fibers of identical shapes in solvents as different as chloroform or toluene, and water [23, 41, 82]. In other systems, slight solvent changes may be reflected in fiber morphology. For example, diacetylenic phospholipid **22** (Scheme 4) gives single-walled tubules in methanol/water, whereas in ethanol/water or water, the same molecule forms multiple bilayers. Some gelators form twisted or helical ribbons in one solvent whereas they form achiral fibrils in other solvents; the size of the helices can also vary significantly depending on the solvent [83–85].

As mentioned above, fiber formation is generally a kinetically controlled event. It is thus no surprise that the cooling rate of the samples strongly affects fiber morphology. Thus, the size of the tubules formed by **22** was reported to vary with the cooling rate [86]. With azobenzene-linked cholesterol derivatives, it was observed that fast cooling of the solution in cyclohexane leads to a mixture of right-handed and left-handed helices, whereas slow cooling gives homochiral helices [87].

Morphology evolution with time has been reported. As explained in Fig. 5, tubular morphology may be derived from the growth of a helical ribbon, and such transitions have often been observed experimentally [65, 88]. Going from tubules to ribbons is also possible. In a mixture of diacetylenic

phospholipid **22** and a short-chain lipid (1, 2-bis(dinonanoyl)-*sn*-glycero-3-phosphocholine), a gradual transformation of nanotubules into a lipid gel phase consisting of interconnected "helical" ribbons (i.e., twisted ribbons as defined in Fig. 1) was observed at room temperature upon polymerization of the diacetylenic functions [89].

Small changes of the chemical structures also lead to strong changes of chiral aggregate morphology. Typical molecular parameters that induce significant morphology variation are the length [55, 87, 90, 91] and the number of unsaturations [68] of alkyl chains. In the case of bolaamphiphiles [92–94], not only the length of the spacer alkyl group matters but also whether it has an odd or an even number of carbon atoms, as revealed by IR spectroscopy (Fig. 7). With the salts of L- and D-12-hydroxystearic acid **26** (Scheme 4) mentioned above [37, 58, 59], the nature of the cation affects helix handedness: Rb^+ and Cs^+ salts give a handedness opposite to that of Li^+ salts, and Na^+ and K^+ salts give a mixture of both right- and left-handed helices [95]. As an example of the delicate balance that determines whether twisted or helical ribbons are formed, the former were obtained from a long-chain glutamate lipid with an oligosarcosine head group, whereas the lipids with an oligoproline head group gave the latter [96]. It is interesting to note that these changes in fiber morphology do not necessarily affect significantly the gelling properties (gel aspect, gel stiffness, or gelling temperature).

Diastereomers can have highly variable and unpredictable behaviors as demonstrated by the n-alkyl aldonamide-derived lipids [32, 64]. An alkyl galactonamide derivative forms helical ribbons whereas the mannonamide derivative forms a rolled-up sheet, and the gluconamide derivative forms multiple helices. Mixtures of these three aldonamides with various chain lengths showed that they may coaggregate or aggregate separately depending on their absolute and relative configurations, and on the difference in alkyl chain length. The functionalization of these alkyl aldonamides also has strong effects on the morphology of their aggregates [84, 97].

The various relations that can be established between molecular chirality and fiber handedness are worth a detailed presentation. The general rule is that the handedness of a chiral self-assembled fiber is controlled by the stereochemistry of the molecule. One enantiomer gives a right-handed fiber and the other enantiomer a left-handed fiber. However, there are some rare cases where a pure enantiomer of a chiral molecule assembles into a mixture of right- and left-handed helices. This is the case for the phosphonate analogues of diacetylenic lipid **22** (Fig. 8) [98–100], for cholesteryl anthryloxybutanoate [83], or for a mixture of a bile salt, a phosphatidylcholine, and cholesterol (Fig. 9) [101]. In the latter case, in addition to the fact that both right- and left-handed helical ribbons are observed, two or three different and well-defined helical pitches coexist (Fig. 9) [101].

Sometimes, even achiral molecules can form helical fibers: achiral isomers of diacetylenic lipid **22** (Fig. 10) [102], cyanurate derivatives [103],

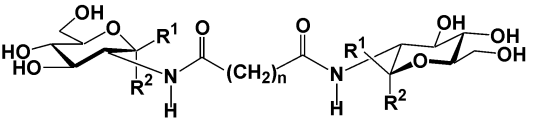

(n = 9, 10, 11, 12, 13, 14, 16, and 18)

1(n) : R^1 = H, R^2 = OH (α-anomer)
R^1 = OH, R^2 = H (β-anomer)

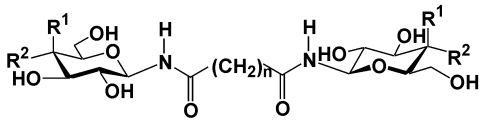

2(n) : R^1 = H, R^2 = OH; n = 6, 9, 10, 11, 12, 13, and 14

3(n) : R^1 = OH, R^2 = H; n = 10, 11, and 12

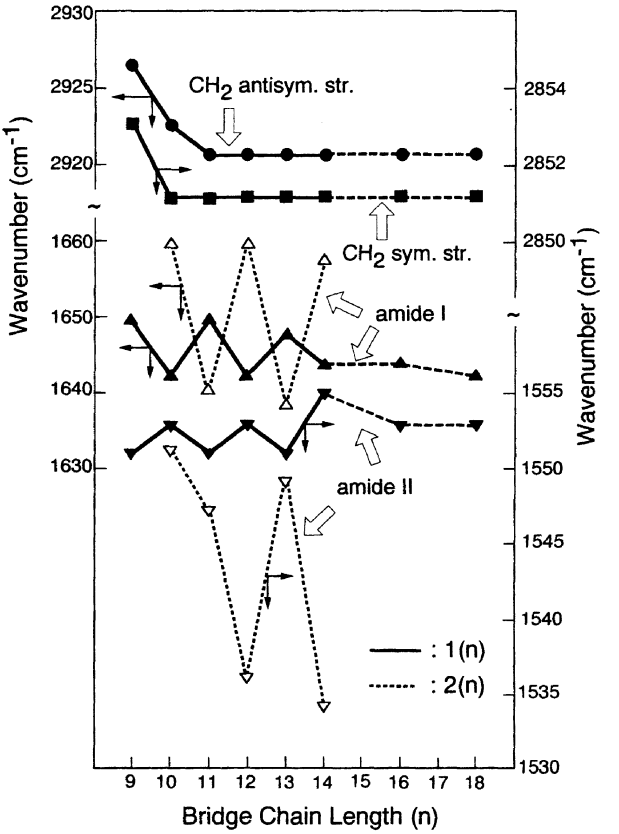

Fig. 7 Dependence of IR band frequencies on the spacer length (n) of glucosamide bolaamphiphiles. Reprinted with permission from [93]. Copyright 1999 American Chemical Society

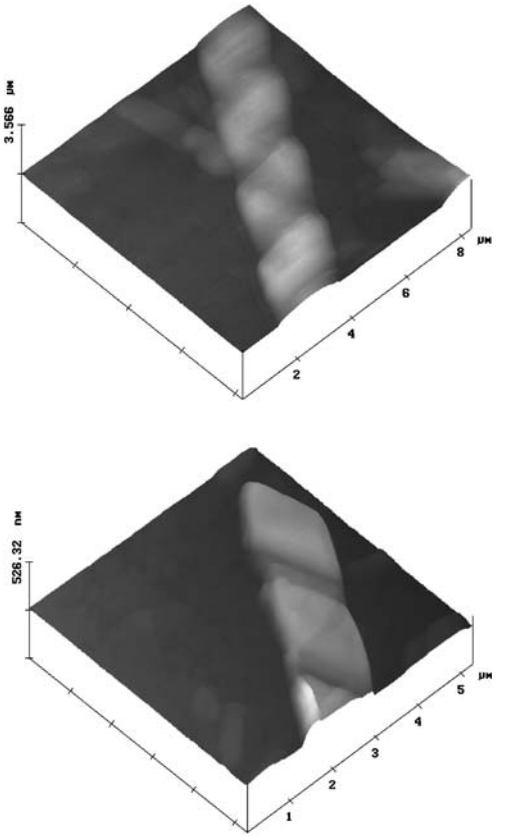

Fig. 8 Contact-mode AFM images of diacetylenic phosphonate lipids showing the presence of both right- and left-handed helices with a pure enantiomer of the lipid. Reprinted with permission from [98]. Copyright 1998 American Chemical Society

some cyanine dyes [104, 105], perfluorinated lipids [106, 107], and various bolaforms [108–110]. In the case of a family of nucleobase-derived bolaamphiphiles, nonchiral bis-thymine bolaamphiphiles form double-helical ropes (Fig. 11) whereas bis-adenine bolaamphiphiles only form microcrystalline solids [110]. A mixture of bis-thymine and bis-adenine or thymine–adenine bolaamphiphiles yield nonchiral nanofibers. It was suggested that bis-thymine bolaamphiphiles may photodimerize leading to chiral molecules which may, in turn, pack in a chiral way. Assembly of the same molecules in the dark did not yield helical structures.

To finish this section, additives or mixtures in various proportions have also been used to tune chiral aggregate morphologies. For example, a transition from twisted ribbons to helical ribbons has been observed in mixtures of cardanyl glucosides with saturated and unsaturated alkyl chains [68]. When

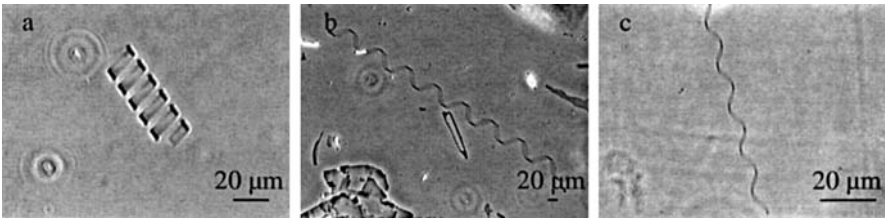

Fig. 9 Three different helical pitches observed with a mixture of a bile salt, phosphatidylcholine, and cholesterol. The pitch angle is **a** $11 \pm 2\,^{\circ}$, **b** $54 \pm 2\,^{\circ}$, and **c** $40.8 \pm 2\,^{\circ}$. Reprinted with permission from [101]. Copyright 1999 National Academy of Sciences USA

the relative proportion of the unsaturated derivatives is increased, twisted ribbons change into helical ribbons and then tubules. The diameter of the tubules formed by diacetylenic lipid **22** can be reduced by a factor of 10 upon adding a short-chain phospholipid [89]. For the same lipid, it was observed that the presence of a few percent of negatively charged lipids yields tubules with three different pitch angles, 14, 28, and 42°, and with diameters of 2000–2500, 1000–1500, and 700–1000 nm, respectively [111]. These results can be compared to what was observed with the bile system presented above [101].

As discussed in Sects. 2.3 and 2.4, mixing the two enantiomers generally results in important changes in fiber morphology. Racemates tend to form platelets that do not express any chirality. In a couple of cases [35, 36] as, for example, for diacetylenic lipid **22** [33, 34], a mixture of right-handed and left-handed helices is observed instead of platelets. Data are rarely available concerning the behavior of mixtures of enantiomers other than 1:1 racemic mixtures. In the case of diacetylenic lipid **22**, the phase separation between the enantiomers should lead to tubules of opposite handedness, the propor-

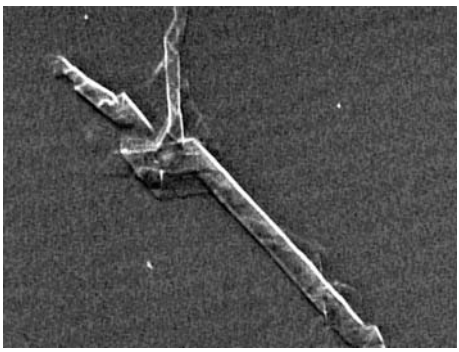

Fig. 10 Chiral tubular structure formed by an achiral β-lecithin molecule. No handedness preference is shown. The width of the image is about 8 µm. Reprinted with permission from [102]. Copyright 2003 National Academy of Sciences USA

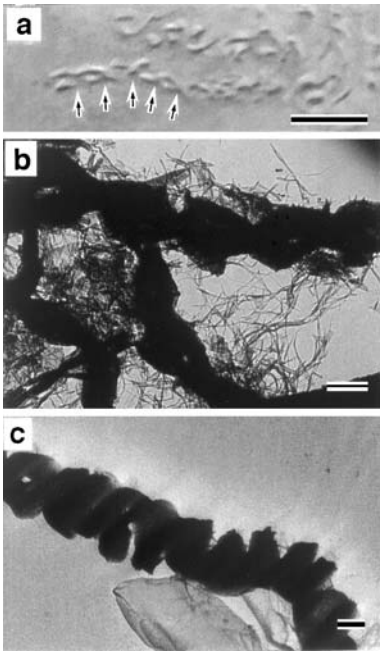

Fig. 11 Double-helical ropes of achiral bis-thymine bolaamphiphiles. Reprinted with permission from [110]. Copyright 2001 American Chemical Society

tions of which reflect the overall proportion of enantiomers (Fig. 12). In the case of cationic bis-quaternary ammonium gemini amphiphiles with tartrate counterions **23** (Scheme 4), studies of aggregate morphology as a function

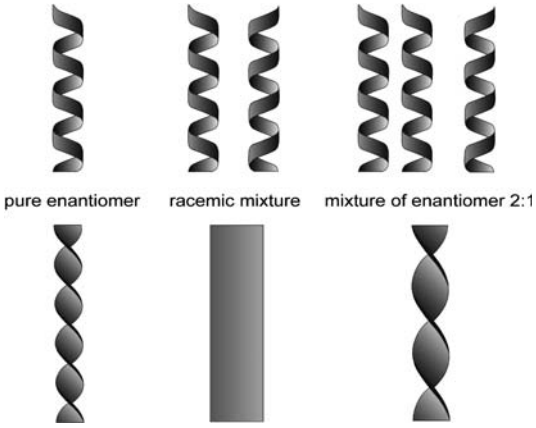

Fig. 12 Schematic representation of the effect of the proportion of enantiomers (*top*), and the case of continuous mixing of the enantiomers (*bottom*) as in a solid solution [43]

of enantiomer proportions showed that increasing the enantiomeric excess from 0 (racemic) to 1 (pure enantiomer) results in a continuous decrease of the pitch of the twisted fibers from infinite (flat ribbons) to about 200 nm (Fig. 12) [43]. This behavior may be due to the unique features of this system; the chirality belongs to the counterion and not to the amphiphile itself, but a conformationally labile chirality can be induced in the structure of the amphiphile [112]. Up to now, such continuous pitch variation has not been observed in any other system.

3.3 From Molecular Chirality to Supramolecular Chirality: Molecular Organization in Chiral Fibers

The helical pitch of twisted or helical fibers or ribbons typically ranges from ten nanometers to microns. This means that the number of molecules needed to span one turn of a helix lies between hundreds to tens of thousands. In other words, the twist between a molecule and its neighbor associated with fiber helicity will be at most one degree and, very often, much less than that. This change of scale of chirality and the cooperative effects that are involved are not easily understood. A number of theoretical models have been proposed to explain the formation of chiral fibers, among which those about cylindrical tubules and helical and twisted bilayer ribbons are probably the most elaborate. These models have been presented in detail in several reviews and we will simply refer the reader to these [4, 67, 113]. Theories are successful in describing some chiral fiber morphologies by introducing chirality as a global parameter. However, they treat the system as a continuous medium instead of an ensemble of discrete chiral molecular objects having a specific shape. Thus, they do not allow prediction of the behavior of a given molecular system under given experimental conditions.

From an empirical perspective, several factors have been pointed to as necessary for designing molecules that self-assemble into fibers with chiral morphologies, besides the presence of stereogenic centers. Such molecules are most often "amphiphilic". This term is understood here in its broadest sense. It implies that the molecules are composed of two antagonist parts. One is solvophobic and provides the driving force for aggregation; the other is solvophilic and assures the solubilization of the amphiphile and the stability of the aggregates in suspension. Additionally, the molecules possess some chemical functions capable of directed noncovalent interactions and/or rigid segments which determine the pseudocrystalline organization of the molecules in the fibrous structures. Thus, small molecules that assemble into chiral fibers often possess hydrogen-bonding functions and may combine amino acid or amide functions [23, 36, 76, 108, 114], sugar groups [21, 22, 69, 74, 115, 116], or both as in gluconamides [28, 32, 84, 97, 117, 118], as well as urea functions [29, 119–121]. Replacing a hydrogen-bonding function by

a non-hydrogen-bonding one, e.g., exchanging an amide for an ester [122], results in a loss of directional interactions and no fibrous aggregate forms. Aromatic $\pi - \pi$ stacking is also commonly involved in fibrous chiral aggregates [16, 26, 36, 65, 69, 74, 123–126]. Among the rare precursors to chiral fibers that possess neither hydrogen-bonding functions nor aromatic groups are diacetylenic phospholipids such as **22**, the helices and tubules of which are among the most extensively studied aggregates [2, 32, 34, 53, 54, 60]. To explain why such molecules form helical ribbons or tubules while other phospholipids do not, it was proposed that diacetylene groups add rigidity and a kink to the alkyl chains, which might impose some steric hindrance when the molecules pack parallel to each other. A chiral twist of the packing allows alleviation of this hindrance [34].

The nature of molecular organization within the aggregates is very important to determining whether and how chirality is transferred from individual molecules to their aggregate structures. But accurate data are still very difficult to obtain. Formally, in order to correlate structural information about packing at the molecular level and information about the morphology at the fiber level, both types of data should be collected simultaneously from the solvated fiber. Correlating the orientation of the molecules with respect to the fiber coordinates in the presence of the solvent is complicated and, in practice, rarely achieved [37, 127]. To date, most studies on molecular organization within fibrous aggregates (chiral or not) have been performed on desolvated fibers, assuming that fibrous aggregates are in a pseudocrystalline state and that molecular organization is unchanged when the gels or the fibers are dried. This assumption is necessary as gels are frequently not amenable to detailed determination of molecular packing, but its validity must be questioned in each case. Thus, wide-angle X-ray powder diffraction or wide-angle X-ray scattering (WAXS) [116, 128], solid NMR [129], and infrared spectroscopy [130] were performed on the desolvated fibers and the results extrapolated to the gel structure. Such measurements can provide information about molecular organization at close to atomic resolution if (and only if) the molecules have crystalline order. Even with this, it remains difficult to propose a correct orientation of the molecules within an individual fiber. Techniques which allow the direct observation of isolated fibers (i.e., electron microscopy and AFM) do not yet have the necessary resolution to observe molecular organization. Moreover, some limitation may originate in the nature of the samples. For instance, some aggregates are labile in solution, and the molecules within the aggregate may possess significant mobility, especially when there is no other driving force for molecular assembly than hydrophobic effects which impose little directional constraint and allow a high degree of conformational freedom.

An assumption that should also be made carefully is that the packing within the gel fibers is similar to the packing of the gelators or of their analogues in single crystals (see Sect. 2.4). Single-crystal structures determined

by X-ray crystallography provide very accurate information about molecular packing [16, 26, 30, 31, 38, 47–50, 116]. However, while some single-crystal X-ray structures have been validated by comparison with powder diffraction patterns of the gels, this control was not performed in many cases. Occasionally, it was even observed that a single-crystal structure and the corresponding gel structure do not match [129]. Furthermore, even with accurate information at the molecular level, it still is not easy to understand precisely how a given molecular packing gives rise to supramolecular chirality in a fiber.

Sometimes attempts can be made to observe fiber orientation by one technique, and to study molecular orientation in the same fiber by another. In most gels, fibers are at or below the limit of detection of optical microscopy, and are isotropically oriented in the sample. Studies of the properties of a single fiber have been accomplished in very few cases, and only under special circumstances where the fibrous structure was observable by optical microscopy (wavelength in the visible range) and when molecular packing within this fiber could be identified from single-crystal structures [127] or by infrared spectroscopy [130]. However, in none of these cases was chirality involved. A more attractive alternative to determine the orientation of the fibers without having to isolate one is to apply an external force or field that induces the aggregates to orient at the moment of their formation. There are many examples of such orientation induction on elongated supra/macromolecular structures in the literature using electric fields [131–136], magnetic fields [137, 138], or by applying a shear field. These have been applied extensively to flexible objects such as wormlike micelles, disklike assemblies, or polymer solutions. Because the fibers in gels are often mechanically fragile, imposing an orientation to the fibers by an external force or field is not trivial. However, rigid tubules have been aligned through such methods [139–142], which bodes well for the possibility of exploring chiral packing of molecules directly in oriented fibrillar structures.

4
Methods for Probing Chirality in Self-assembled Fibers

4.1
Methods for Probing Chirality at the Molecular Level

Various tools may be used to probe intramolecular and intermolecular interactions and to study molecular packing in self-assembled fibers: infrared or UV/Vis absorption spectroscopy; fluorescence spectroscopy; NMR spectroscopy; X-ray diffraction and X-ray scattering etc. In this section we focus on the techniques that may provide information related to chirality.

Single-crystal X-ray crystallography gives the most complete and accurate description of the conformations and packing of molecules in the solid state. As mentioned in Sects. 2.4 and 3.3, this also applies to chiral gelators whose X-ray structures often show linear arrays of tightly associated molecules suggesting a preferred direction of fiber growth, and 2_1 chiral screw rotation symmetry axes. However, the use of crystallography to study chiral fibers is limited on several grounds. First of all, crystals of gelators suitable for X-ray diffraction are very difficult to obtain, precisely because these molecules tend to aggregate into gel fibers, or at best into thin needles instead of crystals of sizable dimensions. Crystallographic studies are often performed on analogous molecules that possess poor or no gelling abilities. Second, it is very difficult to establish that the linear arrays seen in the crystals define the direction of preferred fiber growth. Moreover, crystals possess a long-range order and by definition show no long-range twist or coiling. Thus, molecular packing in a crystal does not provide much information about the origin of chiral fiber morphologies such as those described in Sect. 3. Wide-angle X-ray scattering may be measured directly on gel fibers. Although the information obtained by this technique does not generally allow an accurate description of molecular packing, it gives some distinctive periodicities that may be compared to and eventually validate an arrangement measured in the crystal.

NMR has sometimes been of some use to assess chiral interactions of small molecule gelators. For example, a selective interaction between chiral tartrate anions and achiral dicationic surfactant head groups in gelator **23** (Scheme 4) results in diastereotopic NMR patterns in the signal of the protons of the head groups [112]. Cross-polarization magic-angle spinning (CPMAS) ^{13}C NMR solid-state spectroscopy may allow characterization of molecular conformations and disorder in the molecular arrangements directly in gel fibers, provided that complementary solution NMR data and solid-state spectra of crystals of related molecules are also available. Such studies have been accomplished on *N*-octylhexonamide supramolecular assemblies [129].

The most versatile tool for studying assemblies of chiral molecules is circular dichroism (CD) spectroscopy. CD measures the differential absorption of right- and left-handed circularly polarized light. CD spectra are generally recorded in the UV/Vis range, but measurements in the short-UV and infrared (see below) are also possible. A CD spectrum amounts to the subtraction of two slightly different spectra and, consequently, CD bands are very weak compared to those of the corresponding absorption spectra. However, the intensity and sign of CD bands are extremely sensitive to changes in the conformation of the molecules in the vicinity of the chromophores to which they are allied. Thus, upon aggregation of chiral molecules into fibrous objects, large changes in CD spectra are commonly observed [143], although the changes are sometimes limited to a simple increase of band intensity [144]. As illustrated in the following, these changes are very practical to determine the onset of aggregation. However, they do not necessarily correspond to dra-

matic changes in the conformation of the molecules and interpretation of CD data should always be made cautiously [145].

CD signals may be induced in nonchiral chromophores (e.g., aromatic groups) provided that a chiral group lies nearby. The magnitude of such induced CD is inversely proportional to the third power of the distance between the chiral group and the chromophore [146] and should thus decline very fast as this distance increases. However, in a self-assembled fiber, a chiral environment may be provided by the chiral packing of the molecules. Induced CD may thus be observed in chromophores remote from any stereogenic centers when the overall packing has a chiral twist. For example, strong CD bands allied to the electronic transitions of diazobenzene moieties are observed in the CD spectrum of **19b** in gel fibers (Scheme 3) [29]. CD bands are also observed in chromophores of molecules that do not possess any chiral center but that coaggregate with [147] (or bind to aggregates of [5, 148]) chiral molecules. Such induced CD signals may emerge in a chiral assembly even though chirality may not be observed at the level of the fiber.

One of the main uses of CD is to monitor self-assembly. For a small molecule gelator, a typical experiment consists in following the CD spectrum from a temperature above T_{gel} to a temperature below T_{gel}. A sharp change in the CD spectrum is often observed at the onset of aggregation which may not coincide exactly with gelation. Indeed, the latter occurs only when assemblies become long enough to entrap the solvent and is associated with an increase of viscosity. Using this method, transition temperatures [68, 149, 150], critical aggregation concentrations [150], and the influence of added ions [150] or of the solvent [82] have been determined. Photochemical reactions within gel fibers and the subsequent changes in molecular organization have also been monitored by CD [151].

As mentioned above, the onset of CD signals does not necessarily imply that a structure exhibiting chirality at a mesoscopic scale has emerged. However, when such a structure exists, CD spectroscopy may be useful to monitor changes in aggregate morphology. This is the case, for example, for the transformation from nanotubes to twisted ribbons observed in mixtures of diacetylenic phospholipid **22** and of a short-chain lipid, 1,2-bis(dinonanoyl)-*sn*-glycero-3-phosphocholine (see Sect. 3.1) [89]. Slight changes in the CD spectrum of tubules of the diacetylenic phospholipid **22** have also been used to determine the number of lipid bilayers in the tubule walls [152].

CD spectroscopy may give insights into whether some chiral molecules mix in the same fibers or, on the contrary, phase separate into different aggregates. In particular, when the two enantiomers of a given gelator are mixed, various behaviors may be expected (see Sect. 2.3). If a complete phase separation of the enantiomers into aggregates of opposite handedness occurs, the CD intensity is expected to vary linearly with the enantiomeric excess (ee) of the mixture. Similarly, if the two enantiomers cocrystallize to form a racemic (nonchiral) crystal, CD will arise from the remaining single enan-

tiomer and a linear dependence of CD intensity on ee is expected. However, if the two enantiomers mix, at least partially, regardless of their proportions, coaggregation may occur with negative or positive cooperativity and it is likely that the CD intensity would deviate from a linear dependence on the ee. Thus, a linear dependence of CD intensity on ee in tubules of chi-

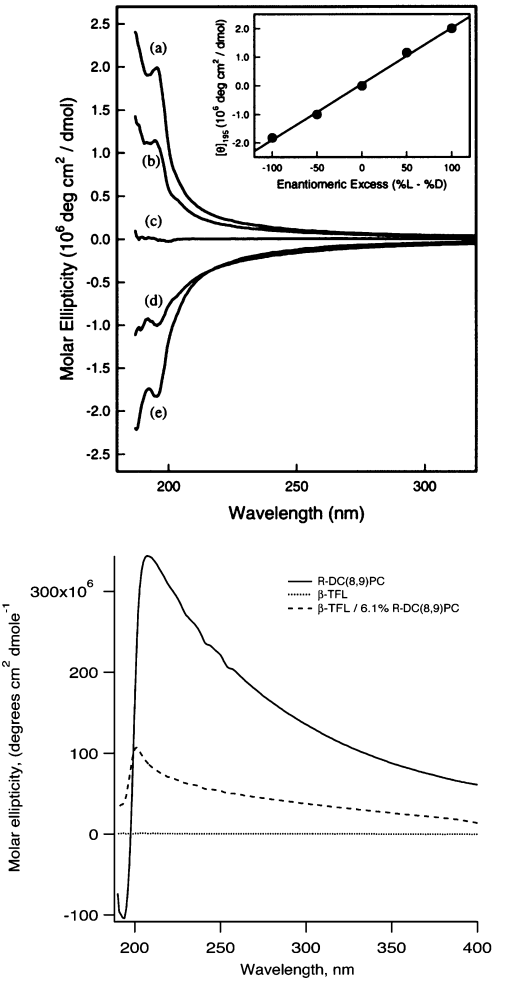

Fig. 13 *Top*: CD spectra of tubules of various mixtures of the two enantiomers of diacetylenic phospholipid **22** (inset: variation of the molar ellipticity as a function of enantiomeric excess) prepared from methanol/water. *Bottom*: CD spectra of tubules of diacetylenic phospholipid **22** (*solid line*), of an achiral analogue (*dotted line*), and of a mixture of the achiral analogue with 6.1% of **22** (*dashed line*). Reprinted with permission from [34] and [102]. Copyrights 1998 American Chemical Society and 2003 National Academy of Sciences (USA)

ral diacetylenic lipids was interpreted as a phase separation (Fig. 13) [34]. This behavior contrasts with that of an achiral diacetylenic lipid that forms equivalent amounts of right- and left-handed tubules. Upon adding only 6% of a similar chiral phospholipid, the intensity of the CD signal increases from zero to approximately 30% of the signal obtained for the enantiopure phospholipids, thus suggesting that the nonchiral lipids may express chirality induced by the added chiral lipid (Fig. 13) [102]. This amplification of chirality by achiral lipids may be compared to the sergeant-and-soldiers effects observed in helical polymers [153]. Other examples of the use of CD spectroscopy to evidence chiral interactions and recognition include the gels of compounds **19a** and **19b** (Scheme 3) [29], and the spontaneous formation of complementary hydrogen-bond pairs of mixtures of melamine and cyanuric acid derivatives and their hierarchical self-assembly in chiral supramolecular membranes [147]. Similarly, CD has been used to study a double-helical arrangement of A–T base pairs in an oligonucleotide-templated self-assembly of nucleotide bolaamphiphiles [154].

It is difficult to draw definite conclusions from a CD spectrum about the conformations of molecules and their relative positions in a gel fiber. The assignment of CD bands to the transitions of the chromophores to which they are allied is not always straightforward because significant bathochromic or hypsochromic shifts may occur upon aggregation; assignments performed from the absorption spectrum in solution may not provide reliable references. However, when this assignment can be made and when artifacts due to potential linear dichroism can be eliminated, the appearance of exciton coupling in the CD spectra may be interpreted to determine the sign (clockwise or counterclockwise) of a chiral twist of the molecular arrangement. In molecules that possess a single chromophore, exciton coupling occurs intermolecularly and arises from close chiral packing of the chromophores in the fibers. The sign of the exciton coupling indicates the relative orientation of the transition moments allied to the CD band. For example, such assignments have been performed for nitro-substituted derivatives of the 4,6-*O*-benzylidene monosaccharides shown in Scheme 2 [82], and for azobenzene-based sugar derivatives [155]. In the latter case, the sense of helicity at the molecular scale determined by CD spectroscopy corresponds to the handedness observed by SEM at the fiber level. However, to fully validate this correspondence, the orientation of the molecules with respect to the fibers should be determined.

Vibrational circular dichroism (VCD) may provide extra information compared to CD in the UV/Vis range. As this technique measures CD in the absorption region of vibrators, it may be helpful to study molecules lacking chromophores. Its use in the study of chiral aggregates is not yet widespread. But since VCD apparatus are now commercially available, there is no doubt that this method will develop progressively. Vibrational absorption and circular dichroism spectra provide richer information and can, in principle, be more easily predicted and assigned than in the electronic excitation range.

An example of the use of VCD was provided in a study of ammonium gemini surfactants bearing chiral tartrate counterions such as **23** (Scheme 4) [112]. These compounds aggregate into chirally twisted ribbons that express the chirality of the counterions despite the fact that the surfactants are not chiral. However, VCD measurements show induced CD bands in the symmetric and antisymmetric stretching modes of the CH_2 groups of the alkyl chains of the achiral cations. This unambiguously demonstrates that the cations adopt chiral conformations in the chiral ribbons, induced by tartrate anions.

4.2 Methods for Probing Chirality at the Fiber Level

Microscopy is by far the most commonly used technique for structural studies of chiral fiber morphologies. Small-angle neutron scattering and small-angle X-ray scattering have occasionally been used to determine some parameters of helical fibers such as the pitch and the width [76]. But microscopy is usually preferred as it provides direct images of the chiral structures. This preference partly contributes to the aesthetic appeal of some micrographs. However, the preparation of samples and the microscopic observations themselves can induce artifacts, leading to false interpretations such as misassignment of helix handedness. In the following, we intend to briefly compare of some of the methods often used to probe chirality at the fiber level, with their advantages and limitations. These methods are divided into three groups: optical microscopy, electron microscopy and derived techniques, and scanning probe microscopy.

Optical microscopy can provide information about the morphology of chiral fibers if their dimensions exceed a few hundred nanometers (0.2 μm is the lower theoretical limit in the wavelength range of visible light). Numerous examples of chiral fibers observed through this technique can be found, as illustrated in Figs. 9 and 14, which show optical micrographs of both helical and twisted ribbons [88, 92, 98, 99, 101, 109].

Despite the relatively limited accessible magnification, optical microscopy offers the possibility of direct observation of the native structures, since it requires *neither* drying *nor* staining, thus reducing the risk of artifacts. It has been demonstrated that sometimes the same solution displays much richer morphism of chiral structures when probed with optical microscopy than with electron microscopy [88]. However, optical microscopy and, more generally, techniques based on transmission observations of three-dimensional structures may be limited when it comes to an unambiguous determination of chiral aggregate handedness. This problem is particularly well described by Thomas et al. [98]. For instance, in the case of helical ribbons, it may be difficult to distinguish the two sides of the ribbon closer to and farther from the microscope objective, making it difficult to distinguish the apparent handedness. This problem may be partially overcome by using Nomarski differential

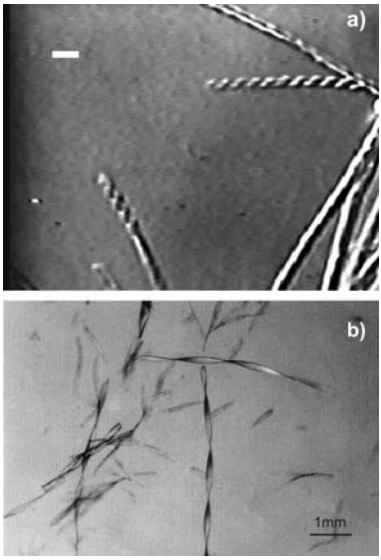

Fig. 14 Optical micrographs of left- and right-handed helical ribbons (**a**) and twisted ribbons (**b**). Reprinted with permission from [99] and [109]. Copyrights 1999 and 2000 American Physical Society and American Chemical Society

interference contrast (DIC) microscopy. This technique has a high sensitivity to the sample thickness, leading to a small focal distance that permits unambiguous placement of the microscope focal plane on either side of the chiral object, provided that the dimensions of the helices allow focalization solely to one side of the ribbons. In this case, one should be very careful about the position of the focus plane to avoid potential confusion (Fig. 15).

As can be noticed from the various figures of Sect. 3, electron microscopy is a very common tool for studying the morphology of chiral fibers. Both scanning (SEM) and transmission (TEM) electron microscopies are used to observe molecular assemblies at much higher resolutions compared to optical microscopy, and allow determination of the morphology and dimensions of chiral structures. However, one must underline the limits of these techniques. First, observations by electron microscopy operated under high vacuum require desolvation or thermal fixation (cryogenic techniques) of the samples. Desolvation of molecular assemblies in solution may cause a collapse or shrinkage of the structures. Moreover, organic molecules in the fibers and the carbon films that support them have a similar electron density. The samples often require staining or metal shadowing to improve contrast. These contrasting methods may cause artifacts for estimating the dimensions of chiral fibers as they result in larger apparent diameters [114]. Additionally, staining with heavy metal salts can modify gelation behaviors [71].

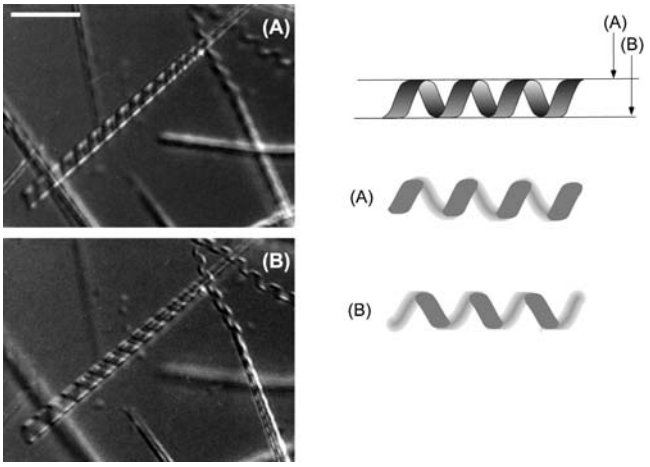

Fig. 15 Optical micrographs through a focus sequence of a large hydrated phosphonate tubule. Illustration of apparent shift in handedness upon changing the height of the focal plane. The scale bar is 5 μm. Photographs reprinted with permission from [98]. Copyright 1998 American Physical Society

Provided these potential artifacts do not affect the chiral morphologies, unambiguous assignment of their right- or left-handedness may still not be straightforward [33, 34, 155] especially when observing negatively stained images by TEM. In the case of negative staining, the total projections do not provide clear information about the orientation of fiber curvature in the plane perpendicular to the sample (Fig. 16). Using appropriate staining methods may help overcome this problem. When carefully contrasting chiral objects with a correct angle, for example using platinum, preferential shadowing can be obtained, thus helping the correct determination of handedness [28].

Finally, the preparation of grids for TEM requires successive steps which should all be performed very carefully to avoid confusion in handedness assignment: (1) deposition of the sample; (2) staining or shadowing; (3) introduction of the grid into the microscope; (4) production of images or of negatives; and (5) scanning or development on paper. At many of these steps, a lack of care in the manipulation will produce the mirror image of the desired micrograph and thus a wrong assignment of handedness (Fig. 17).

Cryogenic techniques have also been successfully used for the study of chiral effects in fibrillar networks. The great difference when using these techniques is that samples undergo an ultrafast freezing to avoid crystallization of the solvent before observation, therefore upholding the native morphologies. This is hardly practical for gels produced in solvents which cannot be frozen in an amorphous state and is most commonly performed

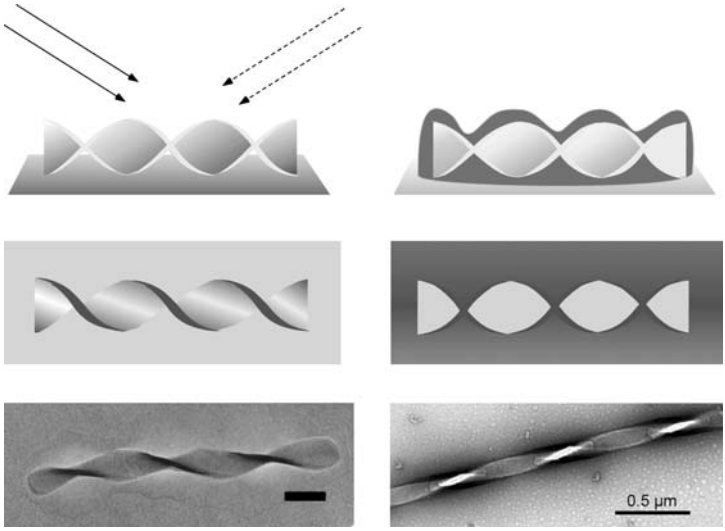

Fig. 16 Metal shadowing (*left*) versus negative staining (*right*). Metal shadowing is deposited to one side of the object along a preferential incidence (*arrow*), allowing easier handedness evaluation. The *bottom left* picture is a Pt shadowed TEM image of a twisted ribbon formed by a mixture of **23** (Scheme 4, $n = 16$) and its analogue bearing bromide counterions. The *bottom right* picture is a TEM image of a twisted ribbon of **23** stained with uranyl acetate with no metal shadowing

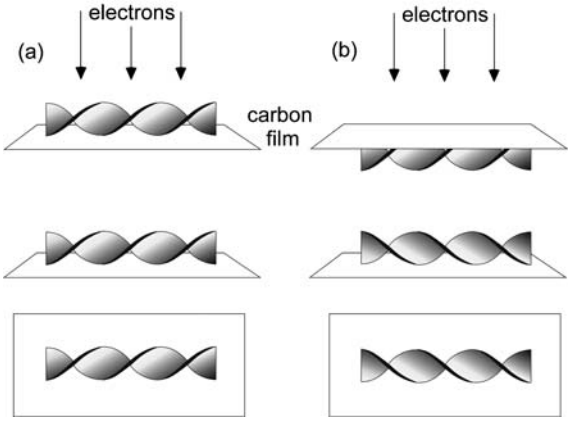

Fig. 17 Effect of sample position on handedness assignment: **a** when electrons hit the helix before the support film (*top*), the original handedness is observed on the micrograph (*bottom*), whereas **b** if the grid is put upside down, the images show an inverted handedness

with aqueous samples. Thus, cryo-TEM has been used to observe twisted fibers [105], as well as twisted [128] or helical [23] ribbons. This technique involves the formation of a thin vitrified film of the solution and the

direct observation of this film, i.e., of the solvated objects, with TEM. An advantage of cryo-TEM is that it does not require staining because of the intrinsic contrast between vitrified ice and organic materials. But this particular feature also constitutes a drawback when studying chiral objects, since the absence of shadowing makes the determination of handedness uncertain (Fig. 18). It should also be mentioned that cryo-TEM is not always well adapted to the study of highly viscous systems such as gels, because of the difficulty of forming a sufficiently thin film with well-defined structures. These are probably the reasons why cryo-TEM observations are often complemented by other measurements, such as TEM on carbon–platinum shadowed samples.

Freeze fracture is another technique associated with TEM. Here, frozen samples are fractured and replicated by carbon–platinum spread at a specific angle under vacuum. Replicas are then observed under standard TEM operating conditions. Due to the shadowing procedure, the images obtained through this technique can provide more accurate information about chiral fiber handedness [56, 118, 149, 156] (Fig. 19). Upon replication, the "topography" of the native sample is conserved leading to 3D images. The handedness of a chiral fiber can then be assigned unambiguously, provided that it can be determined whether a concave or a convex replica is observed. If this latter aspect is not obvious at first sight, the assignment may be facilitated upon slight tilting of the sample grid. Freeze fracture also allows the analysis of viscous samples.

Analogous to freeze fracture, cryo-HRSEM (high-resolution scanning electron microscopy) also permits observation of the sample without prior removal of the liquid phase. Although this technique has been used for the observation of fibrillar structures in gels [157, 158], to the best of our knowledge it has not yet been applied to the study of chiral fibers. However, given the quality of the images that may be obtained, it represents a very promising method for probing the chirality of fibers in solution. Finally, scanning probe microscopies such as AFM or STM also have the potential to image hydrated samples in situ, without desolvation of the fibers, under highly humid conditions (Fig. 20). Yet, examples in the literature generally show dried samples

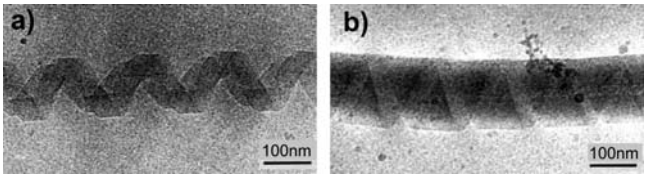

Fig. 18 Cryo-TEM micrographs of helical assemblies in vitrified water: **a** multilamellar helical ribbons; **b** helical ribbons as precursors of tubules. These micrographs illustrate how difficult handedness assignment can be when using cryo-TEM. Reprinted with permission from [23]. Copyright 2001 American Chemical Society

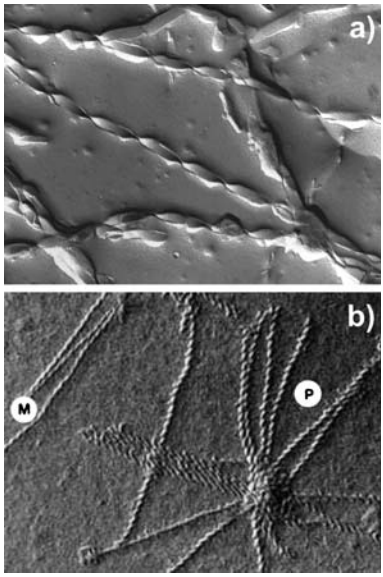

Fig. 19 Freeze-fracture images of **a** twisted ribbons and **b** right- and left-handed helical ribbons. Reprinted with permission from [149] **a** and [156] **b**. Copyrights 2001 and 1990 American Chemical Society

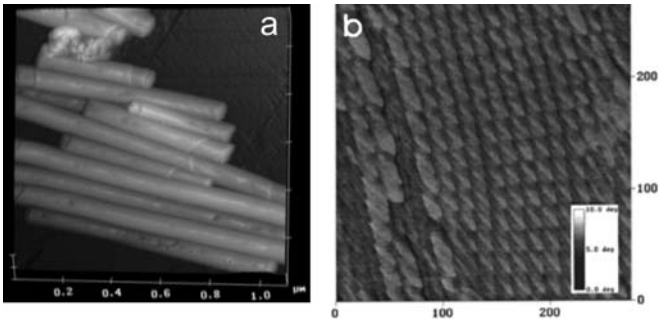

Fig. 20 a AFM image of tubular J-aggregates characterized by a "cigar-like" morphology kindly provided by Prof. H. Von Berlepsch [104]. b High-resolution AFM phase image of quadruple helices. Reprinted with permission from [160]. Copyright 2000 American Chemical Society

that are easier to observe and less mobile. Using these techniques, 3D maps of the samples can be generated that permit unambiguous handedness assignment [99, 159, 160]. However, artifacts may be introduced upon drying. For instance, dried tubules may be so flattened that the images cannot be interpreted with respect to handedness assignment, as for the phosphonate lipid tubules described by Thomas et al. [98] (Fig. 8).

5
Applications and Perspectives

The numerous examples cited in the previous sections illustrate the considerable efforts that have been devoted to the design and characterization of chiral self-assembled fibrillar networks over the last two decades. Supramolecular chemistry has been successful at creating a great diversity of chiral structures with twisted, helical, or cylindrical tubular morphologies that often express the chirality of their molecular constituents at a mesoscopic scale. These chiral structures represent excellent models for studying the emergence of specific shapes at a macroscopic scale through cooperative interactions between a large number of very small building blocks. In addition to this fundamental aspect, they possess a great potential for applications in the development of new functional supramolecular devices, taking advantage of the chirality of the molecular constituents organized in a hierarchical manner or (and) of the supramolecular chirality of the fibers that can be generated.

5.1
Applications Based on Chiral Recognition

Applications of fibers of low molecular weight gelators may emerge directly from the chirality of their molecular constituents. For instance, chiral recognition may occur at the molecular level between various guest molecules and chiral gelators, but only when the latter are engaged in a fiber-like organization. A first example has already been given in Sect. 2 of this chapter: the enantioselective incorporation of (*S*, *S*)-**19b** in the gels of (*R*, *R*)-**19a** (Scheme 3) [29]. Another example is the aqueous gelation of tripodal cholic acid derivative **29** (Scheme 5) reported by Maitra et al. [148]. The gelation of **29** creates highly hydrophobic chiral pockets that recognize the sodium salt of achiral bromophenol blue (BPB; **30**). When the latter is entrapped in the cavities of the gel fibers, circular dichroism bands are observed in the absorption region of BPB, suggesting that chiral conformations are induced in BPB upon recognition. When associating chiral gelators with liquid crystals (LC), original behaviors may also be observed [161]. For instance, cholesteric LC can be induced in the presence of a chiral gel, leading to unique liquid-crystalline physical gels. This topic is presented in detail in the following chapter of this book, and will therefore not be examined further here.

Selective chiral recognition by self-assembled fibrillar networks paves the way to important applications of gels. A first type of application is chiral discrimination/separation: enantioselective elution phenomena using a chiral organic gel as the stationary phase [162]. Chiral stationary phases are normally produced upon grafting chiral groups onto polymer beads. Alter-

natively, the solid-like fibers of a chiral gelator may also be used in chiral separation. This is the case for the benzene gel of a mix of chiral amino acid derived lipids **31a** and **31b** (Scheme 5). Thus, when eluting through this gel an aqueous solution of L- or D-*N*-dansyl-phenylalanine (**32**), a selectivity E_L/*E*_D (*E* = elution rate) of 1.5 was observed. Selective interaction of L-**32** and D-**32** with the gel is supported by the appearance of induced circular dichroism signals of opposite sign belonging to the dansyl chromophore. The intensity of the induced signal is twice as large for the D than for the L enantiomer. Moreover, when a gel of **31a** alone is used as the stationary phase, no enantioselectivity is observed, suggesting that enantioselectivity arises from specific interactions between the positively charged head groups of **31b** with the carboxylate of **32**.

A second potential application of chiral recognition in gel fibers is asymmetric synthesis. Shinkai et al. recently published pioneering work along this line using a derivative of compound **17** [27] as a chiral gelator (Scheme 3) [163]. In fact, they do not use the organic fibers directly. Instead, they use silica inorganic helices produced by replication of the organic fibers (see Sect. 5.3) [164]. Specifically, when applying either left- or right-handed helical silica to the addition of diisopropylzinc to aldehyde **33** (Scheme 6), product **34** is obtained mainly as a single enantiomer (96–98% optical purity). This result is remarkable in that the enantioselectivity of the reaction

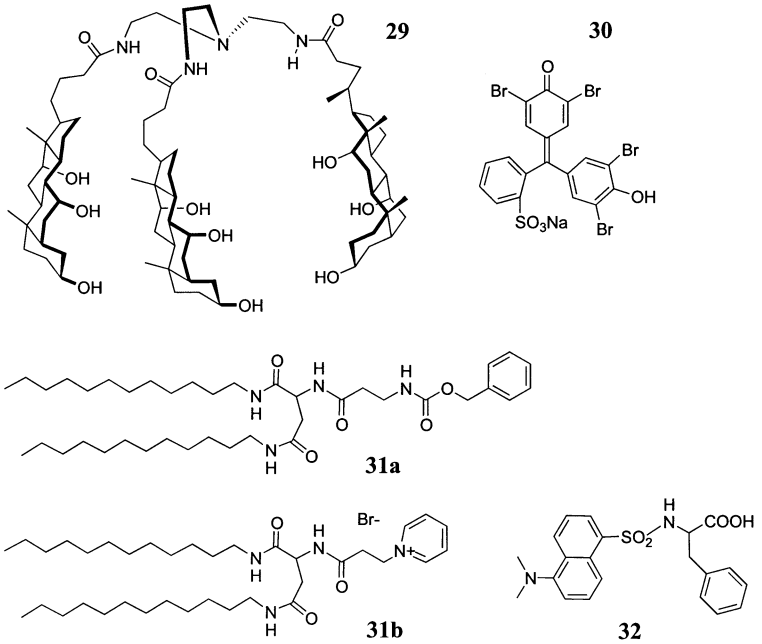

Scheme 5 Molecular components of gels involved in chiral recognition

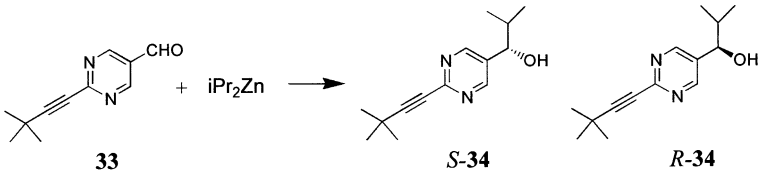

33 *S*-34 *R*-34

Scheme 6 Enantioselective reaction induced by chiral fibers

is not guided by any chiral organic substances, which have all been removed from the silica.

5.2 Chiral Fibers as Templates for Helical Crystallization of Proteins

Chiral fibers can prove potentially useful in biology as templates for the helical crystallization of biological macromolecules. This application is based on the idea that helical crystallization, e.g., of a protein, may be promoted at the surface of tubules formed by self-assembled chiral lipids bearing specific ligands. The helical morphology of the lipid bilayer induces the formation of the tubules and the ligands provide specific binding sites for the protein of interest (Fig. 21). A proof of concept was first proposed by Brisson et al. [165] who showed that biotinylated lipids such as **35** can form unilamellar tubular structures under specific conditions. The biotin residues of the lipids confer the tubules with the ability to recognize the protein streptavidin, which contains four biotin binding sites. Transmission electron micrographs revealed that streptavidin spontaneously assembles into ordered helical arrays on the tubule surface. Importantly, this helical array of streptavidin is induced by the preexisting chiral morphology of the biotinylated lipid tubules. For instance, no organized array of streptavidin was obtained using biotinylated lipids assembled as spheroidal liposomes. Another interesting feature of this system is that these helical crystals of streptavidin now possess biotin binding sites at their periphery. Thus, they may in turn serve as templates to bind a variety of biotinylated molecules. For example, secondary binding of biotinylated ferritin on the streptavidin tubules has been achieved by the authors [165].

Wilson-Kubalek et al. also produced specifically and nonspecifically functionalized unilamellar lipid tubules by using mixtures of a tubule-forming galactosylceramide and various charged or derivatized lipids [166]. Thus, nickel-doped lipids allowed the helical crystallization of histidine-tagged proteins. The authors also reproduced the helical crystallization of streptavidin. They even obtained helical arrays of relatively small proteins, such as actin and annexin, as well as large macromolecules, such as RNA polymerase (Fig. 21).

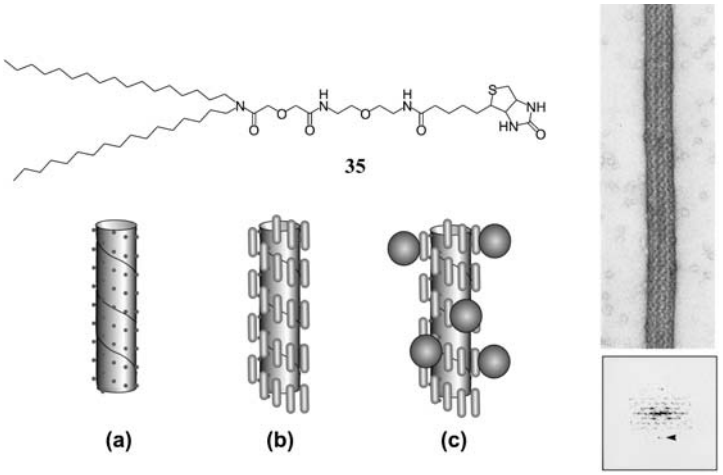

Fig. 21 Structure of biotinylated lipid **35** [165]; schematic representation of the helical crystallization of streptavidin on a chiral tubular structure. **a** Formation of a chiral tubule functionalized with biotin; **b** helical crystallization of streptavidin on the preexisting chiral tubes; **c** secondary binding of biotinylated macromolecules on the remaining binding sites of streptavidin. *Right*: TEM image of a helical array of RNA polymerase on a functionalized ceramide tubule (positive surface charge). The diffraction pattern below, with visible peaks to $1/38\ \text{Å}^{-1}$, illustrates the crystalline nature of the helices. Photographs reprinted with permission from [166]. Copyright 1998 National Academy of Sciences USA

The main advantage of these crystalline helical arrays of proteins is that they represent ideal specimens for 3D electron microscopy. The two-dimensional crystals of proteins at air/water interfaces usually prepared for electron microscopy studies provide a single view of the protein. To allow a 3D structure to be calculated from the images by reconstruction methods, the plane of the crystal can be slightly tilted so as to offer views at different angles. However, this operation requires the recording and combination of many images of tilted specimens and has intrinsic limitations, resulting in the loss of resolution along the direction perpendicular to the crystal plane. On the other hand, the cylindrical symmetry of the helical crystals readily offers all orientations of the repeat motifs. The analysis of helical specimens can be performed using computational tools that have been developed for proteins which spontaneously form helical assemblies, i.e., in the absence of any template. In addition, helical crystals form in solution and can be easily transferred onto electron microscopy grids. In contrast, the transfer of two-dimensional crystals from air/water interfaces is extremely tricky, inefficient, and prone to result in structural damage. Helical crystals may thus be very useful to structure determination.

5.3
Chiral Fibers as Templates for the Growth of Inorganic Replicas

Chiral fibers are representative examples of the variety of shapes, sizes, chemical compositions, and functions that can be reached through the self-assembly of small organic molecules. In contrast, inorganic objects with the same type of morphologies are not readily prepared. One approach to develop inorganic materials closely corresponding to organic assemblies is to transcribe them to produce inorganic replicas by sol–gel methods. Transcription occurs upon adding inorganic derivatives, often metal oxide precursors, to the organic assemblies which may or may not be preformed. Polymerization of the inorganic precursors at the surface of the organic template gives rise to a new robust inorganic material. If the template expresses chirality at a mesoscopic scale, the inorganic replica often does as well. The final product of the transcription process can be an organic–inorganic hybrid or purely inorganic depending on whether or not the organic template has been removed. This approach has developed very rapidly in the last few years. It constitutes a major advance in the design of functionalized materials with applications in the fields of electronics, optics, chromatography, or asymmetric synthesis with, for example, the tailoring of advanced chiral catalysts [163]. Self-assembled organic fibers are very attractive objects for transcription into inorganic materials because their high aspect ratio is expected to produce much sought for rodlike inorganic structures [167]. In the following, we focus mostly on examples where chiral fibers were used as templates. Even so, the literature is already far too rich to make an exhaustive presentation in the context of this chapter, and we have limited the scope of this section to a few examples. For more details, we refer the reader to several review articles [168–170].

Whilst the largest number of transcription protocols of organic templates into inorganic materials have been developed for metal oxides, and in particular silica, some reports deal with metals or semiconductors. Matsui et al. described the electroless metallization of bolaamphiphile nanotubes with nickel and copper baths containing reducing agents, leading to Ni and Cu nanowires that might find applications in nanoelectric circuits (Fig. 22a) [108]. In this case, the bolaamphiphile does not possess any stereogenic center and chirality is not apparent in the inorganic replica. On the other hand, when an achiral precursor gives rise to (both right- and left-handed) twisted ribbons, the twist of the fibers is transcribed into the inorganic replica. For example, a coiled fiber of CdS was obtained in this way (Fig. 22b) [171]. The absence of chirality in the system results in a mixture of right- and left-handed CdS. A remarkable aspect of this process is that CdS grows along only one face of the twisted-ribbon template. The unique coiled morphology of the semiconductor may be suitable for photovoltaic applications [171]. An example of true chirality transfer from organic to in-

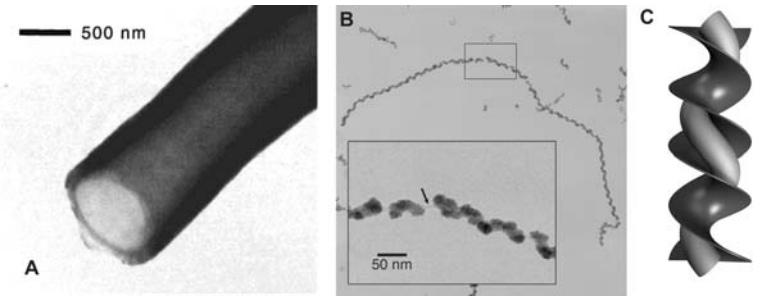

Fig. 22 **a** TEM micrograph of a Ni-coated bolaamphiphile nanotube; **b** TEM micrograph of a helical fiber of CdS with a pitch of 40–50 nm, produced on a twisted-ribbon template as shown in **c**. Reprinted with permission from [108] and [171]. Copyrights 2000 American Chemical Society and 2002 Wiley-VCH

organic structures that is also potentially applicable in the field of electronics and optics is the preparation of helical transition metal oxide tubes, achieved by Hanabusa et al. [172]. Gelator **36** (Fig. 23) is immediately derived from compound **17** [27] (Scheme 3), and possesses positively charged groups that promote the aggregation of the metal oxide precursors at the surface of the gel. Using the two *R*, *R* and *S*, *S* enantiomers of **36**, left-handed and right-handed inorganic helices are produced, respectively.

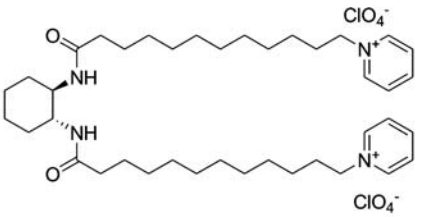

36

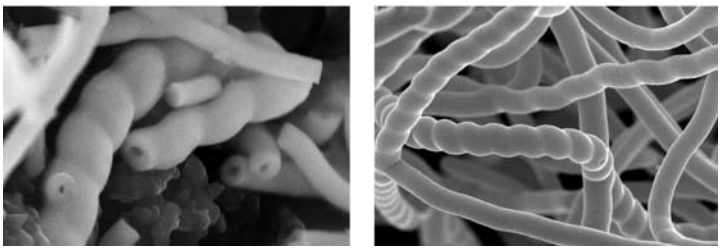

Fig. 23 Structure of **36** and SEM images of tantalum oxide fibers obtained from (*R*, *R*)-**36** (*right*) and (*S*, *S*)-**36** (*left*). Reprinted with permission from [172]. Copyright 2002 American Chemical Society

Tubules and helical ribbons formed by diacetylenic lipids such as **22** (Scheme 4) have been extensively used as templates for metallic coatings [173], and the deposition of gold nanoparticles [174] or polypyrrole threads [175]. Their coassembly with silica precursors gives rise to organic/inorganic hybrids having mesoscopic helical and tubular shapes and multilamellar walls [176].

The largest body of work on transcription of chiral fibers has been devoted to silica because of the ease with which it can be handled. The strong activity the Shinkai research group should be underlined in this respect. Gel fibers can be coated with silica, and yield hollow inorganic tubules after removal of the organic template [177]. If the organic template is hollow in the first place, as in the organic tubules of a crown-appended cholesterol gelator, both the interior and the exterior of the organic tube can be accurately coated with silica, which finally results in double-walled silica tubes (Fig. 24) [178].

Another example of very accurate transcription is the generation of both right- and left-handed silica fibers by sol–gel transcription of helical organogel fibers of a derivative of compound **17** [27] as a chiral gelator (Scheme 3) [164]. The authors clearly established that the final helicity of the inorganic fiber reflects the original chirality of the organic template (Fig. 25). A similar result was obtained with silyl derivatives of gelator **19b** (Scheme 3) [179]. A right-handed helix is produced by the *R*, *R* enantiomer, and a left-handed helix is produced by the *S*, *S* enantiomer. In most examples of helical fiber transcription into silica, the silica precursors are driven to the organic fiber surface by noncovalent interactions. In this case, however, the silica precursors are covalently attached to the gelator.

To illustrate the diversity of chiral inorganic objects that can be obtained by transcription of chiral self-assembled fibers as organic templates, even double-helical silica has been produced. Gels of a mix of sugar-based gelators produce double-helical silica nanotubes by transcription (Fig. 26) [180]. In addition, gels of gemini surfactant **23** (Scheme 4) produce double-helical fibrils of silica [181]. In the latter case, the continuous variation of the pitch

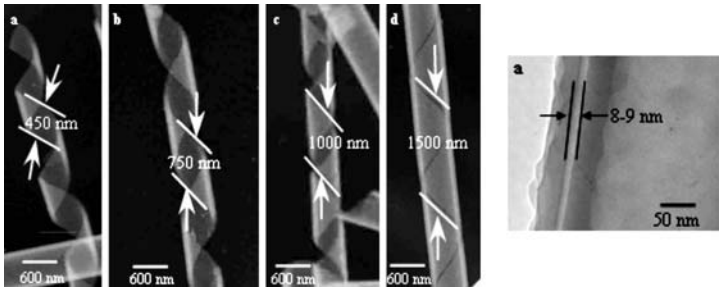

Fig. 24 TEM images of double-walled helical silica obtained after calcination of tubular ribbons in growth. Reprinted with permission from [178]. Copyright 2003 Wiley-VCH

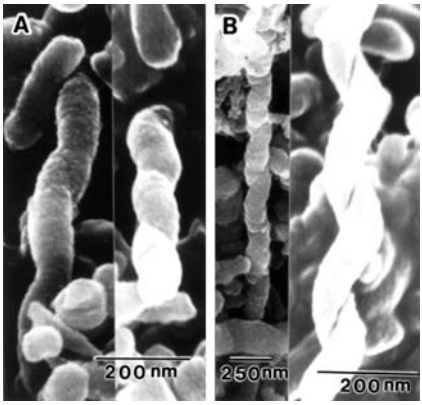

Fig. 25 SEM images of right-handed and left-handed helical silica fibers obtained after transcription of organic chiral templates. Reprinted with permission from [164]. Copyright 2000 American Chemical Society

of the organic template as function of the enantiomeric enrichment of the gelator [43] allows tuning of the pitch of the final double-helical silica.

5.4 Perspectives

The first four sections of this chapter illustrate not only the considerable efforts that have been devoted to the design and characterization of chiral self-assembled fibrillar networks, but also the difficulty in understanding at the molecular scale the mechanisms through which chirality is expressed in self-assembled fibers and how it affects the structure and properties of the gels. To progress along these lines, it will be necessary to gather accurate information about the molecular structure of gel fibers. However, this remains a very challenging task. As is often the case in the chemical sciences, progress may be expected from the improvement of instrumental techniques. The resolution of microscopic tools is still increasing and may reach a level of practical use to distinguish molecules within a fiber. The use of Rietvel methods for X-ray or neutron powder diffraction may lead to the resolution of some gel structures. The improvement of theoretical tools may allow more accurate assignment and interpretation of circular dichroism spectra, both in the electronic absorption range and the vibrational range. Molecular modeling tools have not yet been applied to the study of gel fibers and may also provide useful information.

Future developments will thus aim at understanding how specific shapes assembled from large numbers of much smaller building blocks emerge at a macroscopic scale through cooperative interactions. This fundamental question not only pertains to the science of fibrillar networks, but also to all

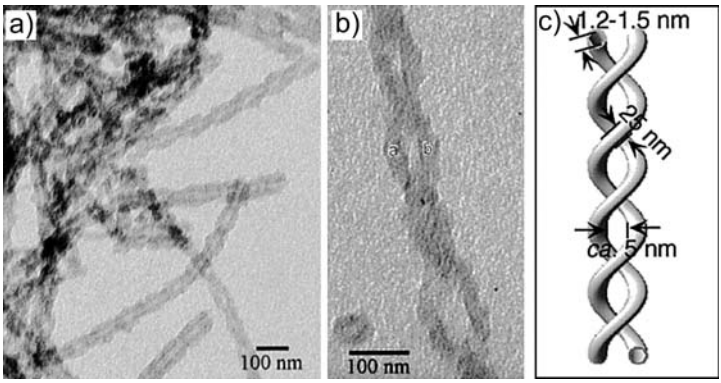

Fig. 26 TEM images **a**, **b** and schematic representation **c** of double-helical silica nanotubes. Reprinted with permission from [180]. Copyright 2002 American Chemical Society

hierarchically organized structures in biology and physics. Answers are not easily found. Yet, applications of these objects have already started to be developed. As seen in this last section, chiral fibrillar networks have proven to be useful in areas as diverse as the helical crystallization of biological macromolecules, chiral separation, and the production of chiral inorganic objects.

References

1. Fuhrhop J-H, Helfrich W (1993) Chem Rev 93:1565
2. Schnur JM (1993) Science 262:1669
3. Kunitake K (1992) Angew Chem Int Ed 31:709
4. Spector MS, Selinger JV, Schnur JM (2003) Chiral molecular self-assembly. In: Green MM, Nolte RJM, Meijer EW, Denmark SE, Siegel J (eds) Materials chirality. Topics in stereochemistry, vol 24. Wiley, Hoboken, NJ
5. Trager O, Sowade S, Bottcher C, Fuhrhop J-H (1997) J Am Chem Soc 119:9120
6. Terech P, Weiss RG (1997) Chem Rev 97:3133
7. Estroff LA, Hamilton AD (2004) Chem Rev 104:1201
8. Luo X, Li C, Liang Y (2000) Chem Commun 2091
9. van Esch J, De Feyter S, Kellog RM, De Shryver F, Feringa BL (1997) Chem Eur J 3:1238
10. Tomioka K, Sumiyoshi T, Narui S, Nagaoka Y, Iida A, Miwa Y, Taga T, Nakano M, Handa T (2001) J Am Chem Soc 123:11817
11. Schoobeek FS, van Esch J, Hulst R, Kellog RM, Feringa BL (2000) Chem Eur J 6:2633
12. Hanabusa K, Koto C, Kimura M, Shirai H, Kakehi A (1997) Chem Lett 429
13. Kölbel M, Menger FM (2001) Chem Commun 275
14. Yasuda Y, Takebe Y, Fukumoto M, Inada H, Shirota Y (1996) Adv Mater 8:740
15. Brotin T, Utermöhlen R, Fages F, Bouas-Laurent H, Desvergnes J-P (1991) Chem Commun 416
16. Babu P, Sangeetha NM, Vijaykumar P, Maitra U, Rissanen K, Raju AR (2003) Chem Eur J 9:1922

17. Lu L, Weiss RG (1996) Chem Commun 2029
18. Terech P, Allegraud JJ, Garner CM (1998) Langmuir 14:3991
19. Saikaigudin Y, Shikata T, Urakami H, Tamura A, Hirata HJ (1987) Electron Microsc 36:168
20. Zana R, Xia J (eds) (2004) Gemini surfactants. Marcel Dekker, New York
21. Yoza K, Amanokura N, Ono Y, Akao T, Shinmori H, Takeuchi M, Shinkai S, Reinhoudt DN (1999) Chem Eur J 5:2722
22. Gronwald O, Shinkai S (2001) Chem Eur J 7:4329
23. Boettcher C, Schade B, Fuhrhop J-H (2001) Langmuir 17:873
24. Bhattacharya S, Ghanashyam Acharya SN, Raju AR (1996) Chem Commun 2101
25. Fuhrhop J-H, Bedurke T, Hahn A, Grund S, Gatzmann J, Riederer M (1994) Angew Chem Int Ed Engl 33:350
26. Mamiya JI, Kanie K, Hiyama T, Ikeda T, Kato T (2002) Chem Commun 1870
27. Hanabusa K, Yamada M, Kimura M, Shirai H (1996) Angew Chem Int Ed Engl 35:1949
28. Fuhrhop J-H, Schnieder P, Rosenberg J, Boekema E (1987) J Am Chem Soc 109:3387
29. de Loos M, van Esch J, Kellog RM, Feringa BL (2001) Angew Chem Int Ed 40:613
30. Jokić M, Makarević J, Žinić M (1995) J Chem Soc Chem Commun 1723
31. Becceril J, Escuder B, Miravet JF, Gavara R, Luis SV (2005) Eur J Org Chem 481
32. Fuhrhop J-H, Boettcher C (1990) J Am Chem Soc 112:1768
33. Singh A, Burke TG, Calvert JM, Georger JH, Herendeen B, Price RR, Schoen PE, Yager P (1988) Chem Phys Lipids 47:135
34. Spector MS, Selinger JV, Singh A, Rodriguez JM, Price RR, Schnur JM (1998) Langmuir 14:3493
35. Gulik-Krzywicki T, Fouquey C, Lehn J-M (1993) Proc Natl Acad Sci USA 90:163
36. Yamada N, Sasaki T, Murata H, Kunitake T (1989) Chem Lett 205
37. Terech P, Rodriguez V, Barnes JD, McKenna GB (1994) Langmuir 10:3406
38. Makarević J, Jokić M, Raza Z, Štefanić Z, Kojić-Prodić B, Žinić M (2003) Chem Eur J 9:5567
39. Watanabe Y, Miyasou T, Hayashi M (2004) Org Lett 6:1547
40. Čaplar V, Žinić M, Pozzo J-L, Fages F, Mieden-Gundert G, Vögtle F (2004) Eur J Org Chem 4048
41. Oda R, Huc I, Candau SJ (1998) Angew Chem Int Ed 37:2689
42. Oda R, Huc I, Candau SJ, MacKintosh FC (1999) Nature 399:566
43. Jacques J, Collet A, Wilen SH (1994) Enantiomers, racemates and resolutions, 3rd edn. Krieger, Malabar, FL
44. Wallach O (1885) Liebigs Ann Chem 286:90
45. Pratt Brock C, Schweizer WB, Dunitz JD (1991) J Am Chem Soc 113:9811
46. Kitaigorodskii AI (1961) Organic chemical crystallography. Consultants Bureau, New York, pp 65–112
47. Makarević J, Jokić M, Perić B, Tomišić V, Kojić-Prodić B, Žinić M (2001) Chem Eur J 7:3328
48. Menger FM, Yamasaki Y, Catlin KK, Nishimi T (1995) Angew Chem Int Ed Engl 34:585
49. Masuda M, Shimizu T (1996) Chem Commun 1057
50. Snijder CS, de Jong JC, Meetsma A, van Bolhuis F, Feringa BL (1995) Chem Eur J 1:549
51. Kinbara K, Hashimoto Y, Sukegawa M, Nohira H, Saigo K (1996) J Am Chem Soc 118:3441

52. Becceril J, Burguete MI, Escuder B, Galindo F, Gavara R, Miravet JF, Luis SV, Peris G (2004) Chem Eur J 10:3879
53. Yager P, Schoen PE (1984) Mol Cryst Liq Cryst 106:371
54. Georger JH, Singh A, Price RR, Schnur JM, Yager P, Schoen PE (1987) J Am Chem Soc 109:6175
55. Yamada K, Ihara H, Ide T, Fukumoto T, Hirayama C (1984) Chem Lett 1713
56. Kulkarni VS, Boggs JM, Brown RE (1999) Biophys J 77:319
57. Sommerdijk NAJM, Lambermon MHL, Feiters MC, Nolte RJM, Zwanenburg B (1997) Chem Commun 1423
58. Tachibana T, Kambara H (1965) J Am Chem Soc 87:3015
59. Tachibana T, Kambara H (1969) Bull Chem Soc Jpn 42:3422
60. Schnur JM, Ratna BR, Selinger JV, Singh A, Jyothi G, Easwaran KRK (1994) Science 264:945
61. McCrea JF, Angerer S (1960) Biochim Biophys Acta 42:357
62. Ramanathan N, Currie AL, Colvin JR (1960) Nature 190:779
63. Nakashima N, Asakuma S, Kim J-M, Kunitake T (1984) Chem Lett 1709
64. Fuhrhop J-H, Schnieder P, Boekema E, Helfrich W (1988) J Am Chem Soc 110:2861
65. Yanagawa H, Ogawa Y, Furuta H, Tsuno K (1989) J Am Chem Soc 111:4567
66. Kunitake T, Yamada N (1986) Chem Commun 655
67. Selinger JV, Spector MS, Schnur JM (2001) J Phys Chem B 105:7158
68. John G, Jung JH, Minamikawa H, Yoshida K, Shimizu T (2002) Chem Eur J 8:5494
69. Jung JH, John G, Masuda M, Yoshida K, Shinkai S, Shimizu T (2001) Langmuir 17:7229
70. Sommerdijk NAJM, Buynsters PJJA, Akdemir H, Geurts DG, Pistorius AMA, Feiters MC, Nolte RJM, Zwanenburg B (1998) Chem Eur J 4:127
71. Fuhrhop J-H, Köning J (1994) Membranes and molecular assemblies: the synkinetic approach. Royal Society of Chemistry, Cambridge
72. Boettcher C, Stark H, van Heel M (1996) Ultramicroscopy 62:133
73. Aggeli A, Nyrkova IA, Bell M, Harding R, Carrick L, Mcleish TCB, Semenov AN, Boden N (2001) Proc Natl Acad Sci USA 98:11857
74. Fuhrhop J-H, Demoulin C, Böttcher C, Köning J, Siggel U (1992) J Am Chem Soc 114:4159
75. Chiruvolu S, Warriner HE, Haranjo E, Idziak SHJ, Rädler JO, Plano RJ, Zasadzinski JA, Safinya CR (1994) Science 266:1222
76. Imae T, Hayashi N, Matsumoto T, Tada T, Furusaka M (2002) J Colloid Interface Sci 225:285
77. Engelkamp H, Middelbeek S, Nolte RJM (1999) Science 284:785
78. Takafuji M, Ihara H, Hirayama C, Hachisako H, Yamada K (1995) Liq Cryst 18:97
79. Lu L, Cocker TM, Bachman TE, Weiss RG (2000) Langmuir 16:20
80. Wang R, Geiger C, Chen L, Swanson B, Whitten DG (2002) J Am Chem Soc 122:2399
81. Lyon RP, Atkins WM (2001) J Am Chem Soc 123:4408
82. Gronwald O, Shinkai S (2001) J Chem Soc Perkin Trans 2 1933
83. Lin Y-C, Kachar B, Weiss RG (1989) J Am Chem Soc 111:5542
84. Hafkamp RJ, Feiters M, Nolte RJM (1999) J Org Chem 64:412
85. Koumoto K, Yamashita T, Kimura T, Luboradzki T, Shinkai S (2001) Nanotechnology 12:25
86. Thomas B, Safinya CR, Plano RJ, Clark NA (1995) Science 267:1635
87. Murata K, Aoki M, Suzuki T, Harada T, Kawabata H, Komori T, Ohseto F, Ueda K, Shinkai S (1994) J Am Chem Soc 116:6664
88. Nakashima N, Asakuma S, Kunitake T (1985) J Am Chem Soc 107:509

89. Svenson S, Messersmith PB (1999) Langmuir 15:4464
90. Hanabusa K, Maesaka Y, Kimura M, Shirai H (1999) Tetrahedron Lett 40:2385
91. Becerril J, Burguete MI, Escuder B, Luis SV, Miravet JF, Querl M (2002) Chem Commun 738
92. Shimizu T, Masuda M (1997) J Am Chem Soc 119:2812
93. Nakazawa I, Masuda M, Okada Y, Hanada T, Yase K, Asai M, Shimizu T (1999) Langmuir 15:4757
94. Schnieder J, Messerschmidt C, Schulz A, Gnade M, Schade B, Luger P, Bombicz P, Hubert V, Fuhrhop J-H (2002) Langmuir 16:8575
95. Tachibana T, Kayama S, Takeno H (1972) Bull Chem Soc Jpn 45:415
96. Shimizu T, Hato M (1993) Biochim Biophys Acta 1147:50
97. Hafkamp RJ, Kokke BPA, Danke IM, Geurts HPM, Rowan AE, Feiters M, Nolte RJM (1997) Chem Commun 545
98. Thomas BN, Corcoran RC, Cotant CL, Lindemann CM, Kirsch JE, Persichini PJ (1998) J Am Chem Soc 120:12178
99. Thomas BN, Lindemann CM, Clark NA (1999) Phys Rev E 59:3040
100. Thomas BN, Lindemann CM, Corcoran RC, Cotant CL, Kirsch JE, Persichini PJ (2002) J Am Chem Soc 124:1227
101. Zastavker YV, Asherie N, Lomakin A, Pande J, Donovan JM, Schnur JM, Benedek GB (1999) Proc Natl Acad Sci USA 96:7883
102. Pakhomov S, Hammer RP, Mishra BK, Thomas BN (2003) Proc Natl Acad Sci USA 100:3040
103. Yang W, Chai X, Chi L, Liu X, Cao Y, Lu R, Jiang Y, Tang X, Fuchs H, Li T (1999) Chem Eur J 5:1144
104. von Berlepsch H, Kirstein S, Böttcher C (2003) J Phys Chem B 107:9646
105. von Berlepsch H, Böttcher C, Ouart A, Regenbrecht M, Akari S, Keiderling U, Schnablegger H, Dähne S, Kirstein S (2000) Langmuir 16:5908
106. Giuleri F, Krafft M-P, Riess JG (1994) Angew Chem Int Ed Engl 33:1514
107. Giuleri F, Guillod F, Greiner J, Krafft M-P, Riess JG (1995) Chem Eur J 2:1335
108. Matsui H, Pan S, Gologan B, Jonas SH (2000) J Phys Chem B 104:9576
109. Lindsell WE, Preston PN, Seddon JM, Rosair GM, Woodman TA (2000) Chem Mater 12:1572
110. Shimizu T, Iwaura R, Masuda M, Hanada T, Yase K (2001) J Am Chem Soc 123:5947
111. Lvov YM, Price RR, Selinger JV, Singh A, Spector MS, Schnur JM (2000) Langmuir 16:5932
112. Berthier D, Buffeteau T, Léger J-M, Oda R, Huc I (2002) J Am Chem Soc 124:13486
113. Selinger JV, MacKintosh FC, Schnur JM (1996) Phys Rev E 53:3804
114. Imae T, Takahashi Y, Muramatsu H (1992) J Am Chem Soc 114:3414
115. Tachibana T, Mori T, Hori K (1980) Bull Chem Soc Jpn 53:1714
116. Shirakawa M, Kawano S, Fujita N, Sada K, Shinkai S (2003) J Org Chem 68:5037
117. Svenson S, Köning J, Fuhrhop J-H (1994) J Phys Chem 98:1022
118. König J, Boettcher C, Winkler H, Zeitler E, Talmon Y, Fuhrhop J-H (1993) J Am Chem Soc 115:693
119. van Esch J, Schoonbeek F, de Loos M, Kooijman HL, Spek A, Kellog RM, Feringa BL (1999) Chem Eur J 5:937
120. Estroff LA, Hamilton AD (2000) Angew Chem Int Ed 39:3447
121. Wang G, Hamilton AD (2003) Chem Commun 310
122. Ihara H, Yamagishi M, Takafuji M, Hachisato H, Hirayama C, Yamada K (1990) Nippon Kagaku Kaishi 1047
123. Nakashima T, Kimizuka N (2002) Adv Mater 14:1113

124. Sagawa T, Fukugawa S, Yamada T, Ihara H (2002) Langmuir 18:2002
125. Yun YJ, Park SM, Kim BH (2003) Chem Commun 254
126. Itojima Y, Ogawa Y, Tsuno K, Handa N, Yanagawa H (1992) Biochemistry 31:4757
127. Abdallah DJ, Sirchio SA, Weiss RG (2000) Langmuir 16:7558
128. Estroff LA, Leiserowits L, Addadi L, Weiner S, Hamilton AD (2003) Adv Mater 15:39
129. Svenson S, Kirste B, Fuhrhop J-H (1994) J Am Chem Soc 116:11969
130. Placin F, Desvergne J-P, Belin C, Buffeteau T, Desbat B, Ducasse L, Lassègues J-C (2003) Langmuir 19:4563
131. Hoffmann H, Krämer U, Thurn H (1990) J Phys Chem 92:2027
132. van der Schoot P, Cates ME (1994) J Chem Phys 101:5040
133. Lachenmayer K, Oppermann W (2002) J Chem Phys 116:392
134. Hong MK, Narayan O, Goldstein R, Shyamsunder E, Austin RH, Fisher DS, Hogan M (1992) Phys Rev Lett 68:1430
135. Oizumi J, Kimura Y, Ito K, Hayakawa R (1996) J Chem Phys 104:9137
136. Oda R, Lequeux F, Mendes E (1996) J Phys II (France) 6:1429
137. Prosser SR, Hunt SA, DiNatale JA, Vold RR (1996) J Am Chem Soc 118:269
138. Katsaras J, Donaberger RL, Swainson IP, Tennant DC, Tun Z, Vold RR, Prosser RS (1997) Phys Rev Lett 78:899
139. Rosenblatt C, Yager P, Schoen P (1987) Biophys J 52:295
140. Terech P, de Geyer A, Struth B, Talmon Y (2002) Adv Mater 14:495
141. Shklyarevskiy IO, Jonkheijm P, Christianen PCM, Schenning APHJ, Del Guerzo A, Desvergne J-P, Meijer EW, Maan JC (2005) Langmuir (in press)
142. Lescanne M, Colin A, Mondain-Monval O, Heuzé K, Fages F, Pozzo J-L (2002) Langmuir 18:7151
143. Xing B, Yu C-W, Chow K-H, Ho P-L, Fu D, Xu B (2002) J Am Chem Soc 124:14846
144. Mukhopadhyay S, Maitra U, Ira Krishnamoorthy G, Schmidt J, Talmon Y (2004) J Am Chem Soc 126:15905
145. Glattli A, Daura X, Seebach D, van Gunsteren WF (2002) J Am Chem Soc 124:12972
146. Craig DP, Power EA, Thirunamachandran T (1974) Chem Phys 27:149
147. Kawasaki T, Tokuhiro M, Kimizuka N, Kunitake T (2001) J Am Chem Soc 123:6792
148. Maitra U, Mukhopadhyay S, Sarkar A, Rao P, Indi SS (2001) Angew Chem Int Ed 40:2281
149. Spector MS, Singh A, Messersmith PB, Schnur JM (2001) Nano Lett 1:375
150. Ihara H, Sakurai T, Yamada T, Hashimoto T, Takafuji M, Sagawa T, Hachisako H (2002) Langmuir 18:7120
151. de Jong JJD, Lucas LN, Kellog RM, van Esch JH, Feringa BL (2004) Science 304:278
152. Spector MS, Easwaran KRK, Jyothi GJ, Selinger JV, Singh A, Schnur JM (1996) Proc Natl Acad Sci USA 93:12943
153. Green MM, Reidy MP, Johnson RJ, Darling G, O'Leary DJ, Willson G (1989) J Am Chem Soc 111:6452
154. Iwaura R, Yoshida K, Masuda M, Oshini-Kameyama M, Yoshida M, Shimizu T (2003) Angew Chem Int Ed 42:1009
155. Kobayashi H, Friggeri A, Koumoto K, Amaike M, Shinkai S, Reinhoudt DN (2002) Org Lett 4:1423
156. Fuhrhop J-H, Svenson S, Boettcher C, Rossler E, Vieth H-M (1990) J Am Chem Soc 112:4307
157. Menger FM, Caran KL (2000) J Am Chem Soc 122:11679
158. Menger FM, Peresypkin AV (2003) J Am Chem Soc 125:5340
159. Marini DM, Hwang W, Lauffenburger DA, Zhang S, Kamm RD (2002) Nano Lett 2:295

160. Messerschmidt C, Svenson S, Stocker W, Fuhrhop J-H (2000) Langmuir 16:7445
161. Moriyama M, Mizoshita N, Yokota T, Yokota T, Kishimoto K, Kato T (2003) Adv Mater 15:1335
162. Ihara H, Shudo K, Hirayama C, Hachisako H, Yamada K (1996) Liq Cryst 20:807
163. Sato I, Kadowaki K, Urabe H, Jung JH, Ono Y, Shinkai S, Soai K (2003) Tetrahedron Lett 44:721
164. Jung JH, Ono Y, Hanabusa K, Shinkai S (2000) J Am Chem Soc 122:5008
165. Ringler P, Müller W, Ringsdorf H, Brisson A (1997) Chem Eur J 3:620
166. Wilson-Kubalek EM, Brown RE, Celia H, Milligan RA (1998) Proc Natl Acad Sci USA 95:8040
167. Xia Y, Yang P, Sun Y, Wu Y, Mayers B, Gates B, Yin Y, Kim F, Yan H (2003) Adv Mater 15:353
168. Van Bommel KJC, Friggeri A, Shinkai S (2003) Angew Chem Int Ed 42:980
169. Mann S, Burkett SL, Davis SA, Fowler CE, Mendelson NH, Sims SD, Walsh D, Whilton NT (1997) Chem Mater 9:2300
170. Jung JH, Shinkai S, Shimizu T (2003) Chem Rec 3:212
171. Sone ED, Zubarev ER, Stupp SI (2002) Angew Chem Int Ed 41:1706
172. Kobayashi S, Hamasaki N, Suzuki M, Kimura M, Shirai H, Hanabusa K (2002) J Am Chem Soc 124:6550
173. Schnur JM, Price R, Schoen P, Yager P, Calvert JM, Georger J (1987) Thin Solid Films 152:181
174. Burkett SL, Mann S (1996) Chem Commun 321
175. Goren M, Qi Z, Lennox RB (2000) Chem Mater 12:1222
176. Seddon AM, Patel HM, Burkett SL, Mann S (2002) Angew Chem Int Ed 41:2988
177. Ono Y, Nakashima K, Sano M, Kanekiyo Y, Inoue K, Hojo J, Shinkai S (1998) Chem Commun 1477
178. Jung JH, Lee S, Yoo JS, Yoshida K, Shimizu T, Shinkai S (2003) Chem Eur J 9:5307
179. Moreau JEJ, Vellutini L, Wong Chi Man M, Bied C (2001) J Am Chem Soc 123:1509
180. Jung JH, Yoshida K, Shimizu T (2002) Langmuir 18:8724
181. Sugiyasu K, Tamaru S-I, Takeuchi M, Berthier D, Huc I, Oda R, Shinkai S (2002) Chem Commun 1212